Universidade do Minho
Escola de Engenharia

Gonzalo Padilla Quincot

Measurement of internal moisture distribution in concrete with relative humidity sensors

October 2012

Measurement of internal moisture distribution in concrete with relative humidity sensors
Gonzalo Padilla Quincot
UMinho | 2012

Universidade do Minho
Escola de Engenharia

Gonzalo Padilla Quincot

Measurement of internal moisture distribution in concrete with relative humidity sensors

Master's Dissertation
Integrated Master in Civil Engineering

Work made under the orientation of
Professor Doctor Miguel Ângelo Dias Azenha
And co- orientation of
Professor Doctor Joaquim António Oliveira de Barros

October 2012

ACKNOWLEDGMENTS

I would like to thank Professor Miguel Azenha for the constant support and guide during this research. During the experimental campaign and the thesis write up, Professor Miguel has been always available in spite of his limited time. On the same way, I would like to express my gratitude to Professor Joaquim Barros, who gave me the opportunity to do my studies in Portugal and who also has been always supporting my research.

The research team of the department of civil engineering have been also very supportive, specially the research fellow Christoph de Sousa. I would like to thank him for his support and help during my research. I also express my acknowledgment to the research fellow Jose Granja, who helped me monitoring my experiments in the last stage.

Finally, I would like to thank all the technical team of the laboratory for their support during the concrete preparation and casting, the guidance for the use of the laboratory equipment and their advice for how to develop the experiments.

ABSTRACT

The moisture content in concrete is closely related with its structural behaviour. The cement hydration process is the main responsible for the strength growth development and for heat generation, which in turn induces volumetric changes. Furthermore, the drying process of concrete creates tensile stresses that could lead to an initial stress state build-up and limit the concrete ability to carry further tensile stresses, or generate cracks during service life operating conditions. This is an issue that has been subject of attention of recent design codes but still a lot of research has to be developed to fully understand this behaviour. This is due to the enormous variations that may occur on the concrete compositions and on the in-situ environmental conditions, which makes difficult to predict the actual shrinkage deformations and the role of humidity on it.

On this regard, the study of shrinkage, cracking, moisture loss, thermal deformations and the evolution of the mechanical properties in concrete since casting and throughout the service life are a crucial issue in order to predict the structural behaviour of concrete.

The scope of the present research work is to approach the understanding of the concrete moisture loss process and to contribute with the lack of information in this domain. Different methods of moisture loss measurements inside concrete have been explored but the focus is through relative humidity measurements.

On this regard, the use of different RH sensors and the definition of appropriate monitoring techniques with reasonable accuracy, repeatability and cost-efficiency have been studied. To achieve this, preliminary experiments have to be done to determine the reliability of the measurements and ensure the accurate conditions for the project development. This includes environmental conditions (achieve constant relative humidity environments), sensor and monitoring systems tests, experimental set up with accurate procedures and preliminary measurements in concrete specimens.

Keywords: Relative humidity; humidity sensors; concrete; monitoring; internal moisture distribution.

RESUMO

O conteúdo da humidade no betão está intrinsicamente relacionado com o seu comportamento estrutural. O processo da hidratação do cimento é o principal responsável pelo desenvolvimiento da resistência, e pelas reaccões geradas que resultam em geração de calor causando expansão/contração. Subsequentemente, os processos de secagem do betão induzem alterações volumétricas que podem ocasionar tensões iniciais que, face à resistência à tração do betão pode conduzir à ocorrência de fissuras. Este é um problema que tem vindo a ser tratado nos códigos de projeto, mas o conhecimento dos fenómenos subjacentes e, principalmente a sua codificação em regras de dimensionamento simples, mas efetivas, requer ainda aturada investigação. Tal deve-se à diversidade de composições possível de utilziar no fabrico do betão, bem como a variabilidade de condições ambientais in situ, o que torna difícil estimar as deformações por retração e o papel da humidade neste fenómeno.

Assim, para uma melhor estimativa do comportamento em serviço de estruturas de betão é importante conhecer as deformações que se desenvolvem o risco de fendilhação por retração, a variação de humidade, as deformações de origem térmica e a evolução das propriedades mecânicas do betão desde a sua aplicação.

No presente trabalho pretende-se contribuir para um melhor conhecimento sobre o processo de perda de humidade no betão, tendo-se para tal utilizados diferentes metodologias experimentais de avaliação da humidade relativa interna.

Para tal foram estudados diversos sensores de avaliação de humidade relativa e investigadas várias metodologias de registo deste parâmetro, tendo-se dado especial cuidado à precisão dos registos, sua repetatibilidade e sustentabilidade. Neste sentido, foram efetuados ensaios preliminares de forma a avaliar a fiabilidade dos sensores e as metodologias de medida.

Palavras-Chave: Humidade relativa; sensores de humidade; betão; monitorização; distribução interna do conteúdo da humidade.

INDEX

Acknowledgments ..... **I**

Abstract ..... **III**

Resumo ..... **V**

Index ..... **VII**

Index of Figures ..... **X**

index of Tables ..... **XV**

1 Introduction **1**

2 Methods to measure moisture in concrete **3**

2.1 Methods based on concentration 7

2.1.1 Gravimetric determination 7

2.1.2 Gamma – Densitometry 13

2.2 Methods based on relative humidity 18

2.2.1 Relative humidity measurements embedding sensors in concrete 18

2.3 Equipments for RH measurements in the scope of this research 29

2.3.1 Measuring systems 29

3 Use of salt solutions for assuring constant relative humidity conditions in contained environments **34**

3.1 Sal solutions for humidity calibrators 35

3.2 Experimental program 36

3.2.1 Environmental moisture control in containers 36

3.3 General outline: basic principle and procedure 38

3.3.1 Testing RH sensors and performance of salt solutions for constant relative humidity 38

3.3.2 Test with the same salt (NaCl) 39

3.4 Results and discussion 41

3.4.1 Measurements for the containers with different salts 41

3.4.2 Measurements for the containers with the same salts (NaCl) 45

4 Effect of Gore-tex® protection in moisture measurements 49

4.1 Testing Gore-Tex efficiency 49

4.2 Saturation effect of the sensor after prolonged subjection to very high humidity levels 51

4.2.1 Preliminary test 52

4.2.2 Second test 55

5 Laboratorial experiments regarding humidity profiling in concrete 65

5.1 Moisture loss measurements through relative humidity 65

5.1.1 Experimental set up 65

5.1.2 Sealing the PVC tubes and creating a macro-pore inside the concrete specimens (Latex plug) 70

5.1.3 Sensor tests 75

5.1.4 Preparing the formwork 75

5.1.5 Handling the specimens after casting 76

5.1.6 Relative humidity monitoring 78

5.2 Moisture loss measurements through the gravimetric method (“Slice test”) 79

5.2.1 Expermental set up 79

5.2.2 Create the “Concrete Slices” 79

5.3 Results for relative humidity profiles 81

5.3.1 Specimens A and B 81

5.3.2 Specimen C 85

5.3.3 Specimen D 85

5.3.4 Gravimetric Test 87

5.3.5 Paradela Specimen 88

6 Conclusions 90

7 References 93

INDEX OF FIGURES

Fig. 1. 3D image of pore structure (Kurumisawa and Tanaka 2006) 5

Fig. 2. Water vapour desorption and adsorption isotherms measured at 23°C (Baroghel-Bouny 2007) 6

Fig. 3. Dimension (mm) of specimens subjected to one-face drying (Akita 1996)..... 8

Fig. 4. Profiles of relative water content for one-face drying, where X represent the specimen depth in cm (Akita 1996) 9

Fig. 5. Cylinder with unidirectional moisture flow (Selih 1996) 10

Fig. 6. Schematic representation of the cylinder tested with the PVC meshes (Selih 1994) ... 10

Fig. 7. Moisture content distribution through the depth in the cylinder (a) Experimental results, (b) numerical results; 1 days moist cured lightweight concrete with water/cement ratio of 0.4, at dry period of 0, 1, 3, 7, 28 and 90 days (Selih 1996)..... 11

Fig. 8. Sampling and geometry details of hardened mortar slices (J.C. Amba 2010) 12

Fig. 9. Profiles of free water for mixes MA and MB (J.C. Amba 2010) 13

Fig. 10. Moisture-controlled environment of the beams (S. Multon 2004) 14

Fig. 11. Principle of the gammadensitometry technique (S. Multon 2004)..... 14

Fig. 12. a) Real scale concrete beam b) Gammadensitometry equipment (a: receptacle of the radioactive source, b: receiver for measuring emitted and transmitted flows, c: electric jack connection) (S. Multon 2004)..... 15

Fig. 13. Location of the gammadensitometry sections on a beam and reference marks (S. Multon 2004)..... 16

Fig. 14. Relative mass variation along the upper 300 mm of the beam (S. Multon 2004) 17

Fig. 15. Gamma-ray measurement set-up (Villain and Thiery 2006)..... 17

Fig. 16. Density measured after 1 month of drying (Villain and Thiery 2006) 18

Fig. 17. Capacitive sensor (www.sensirion.com 2009) 19

Fig. 18. Resistivity Sensors (www.conservationphysics.org 2010) 20

Fig. 19. Packaged MEMS sensors (Norris, Saafi et al. 2008) 21

Fig. 20. MEMS response after 24h of curing (Norris, Saafi et al. 2008) 22

Fig. 21. MEMS response after 200 days of curing (Norris, Saafi et al. 2008) 23

Fig. 22. Meniscus shape related with the escape of the water molecules (a) convex, (b) flat (Zachary Grasley 2006) 23

Fig. 23. Evolution of relative humidity in a concrete specimen (Zachary Grasley 2006) 24

Fig. 24. (a)Top view with data acquisition devices (b) Sectional view (Seungwook Lim 2009) 25

Fig. 25. Relative humidity measurements at 25, 75 and 175 mm of the drying cylinder specimen (Seungwook Lim 2009) 25

Fig. 26. Calibration curves for wooden stick and the 95% confidence interval for 112 wooden sticks (Jensen 2003) 27

Fig. 27. Correlation between wooden sticks by use of the desorption curve and AHEAD hygrotemp II sensors (Jensen 2003) 27

Fig. 28. Plastic tube (diameter 2 cm and length 25 cm) mounted with 2 wooden sticks (Jensen 2003) 28

Fig. 29. Humidity profiles of a structure with wooden sticks at (a) 1 m and (b) 3.5 m (Jensen 2003) 29

Fig. 30. Sensirion sensors a) SHT21 and b) SHT71 (www.sensirion.com 2009) 30

Fig. 31. Operating conditions for the SHT21 sensor 31

Fig. 32. Operating conditions for the SHT71 sensor 31

Fig. 33. Honeywell sensors HIH4000 and HIH4010 series 003 and 004 from left to right 32

Fig. 34. Data taker DT515 and CEM20 expansion module 32

Fig. 35. a) VAISALA´s HM44 sensor; b) Data logger 33

Fig. 36. VAISALA HMK 15 relative humidity calibrator (www.vaisala.com 2006) 35

Fig. 37. Containers dimensions (cm) 36

Fig. 38. Sensors ready to place inside the containers 38

Fig. 39. Final distribution of the containers and the installed sensors 39

Fig. 40. Glass and base to be put inside the containers..... 40

Fig. 41. Glasses placed in containers 6 to 9 41

Fig. 42. Relative humidity readings in container 1 (expected relative humidity of 75%) 42

Fig. 43. Relative humidity readings in container 2 (expected relative humidity of 11%) 43

Fig. 44. Relative humidity readings in container 3 (expected relative humidity of 33%) 43

Fig. 45. Relative humidity readings in container 4 (expected relative humidity of 97%) 44

Fig. 46. Relative humidity readings in container 5 (expected relative humidity of 75%) 44

Fig. 47. Relative humidity readings in container 6 (solution for 20 gr of NaCl) 46

Fig. 48. Relative humidity readings in container 7 (solution for 30 gr of NaCl) 46

Fig. 49. Relative humidity readings in container 8 (solution for 40 gr of NaCl) 47

Fig. 50. Relative humidity readings in container 9 (solution for 50 gr of NaCl) 47

Fig. 51. Relative humidity readings in container 10 (solution for 30 gr of NaCl "cooking salt") 48

Fig. 52. Types of Gore-Tex to be used to obtain moisture profiles in concrete 50

Fig. 53. a) Gore-Tex, PVC tube and Latex cork as the sensor´s case; b) Tissue, PVC case and glass of water; c) The tube with the tissue inside blocked with the latex cork on the top and immersed in water; d) After 2 hours the tissue is removed dry 51

Fig. 54. Relative humidity measurements inside water 53

Fig. 55. RH measurements of the sensor with Gore-Tex inside water compared with a free sensor 54

Fig. 56. RH measurements of sensors wrapped with Gore-Tex compared with a free sensor. 55

Fig. 57. Stage 1 - The sensors are placed in the climatic room protected with tape and surrounded with bricks to avoid the wind to disturb the readings..... 57

Fig. 58. Stage 2 - Three sensors were covered with Gore-Tex and one was left free. Sensor S8 directly wrapped, S6 and S7 placed inside the PVC tube and covered with Gore-Tex in two different fashions..... 57

Fig. 59. Stage 3 - The sensors are placed in the same place, surrounded by bricks 57

Fig. 60. Stage 4 - The sensors were placed outside the climatic room, exposed to the environment 58

Fig. 61. Stage 5 - The sensors covered with Gore-Tex were placed each in a glass of water. Sensor S9 was left free 58

Fig. 62. Temperature and RH measurements for 17 days. Three ways of using Gore-Tex: Wrapped, Inverse fashion, Normal fashion 59

Fig. 63. a) Gore-Tex in inverse fashion sealed with silicone; b) Gore-Tex in normal fashion sealed with silicone 61

Fig. 64. 58 days temperature and RH measurements with Gore-Tex in normal fashion, inverse fashion and with one sensor leaved free 62

Fig. 65. Close up of previous figure for a better visibility of the sensor´s behaviour 64

Fig. 66. Specimens A and B 66

Fig. 67. Pocket size proportions for specimens A and B 67

Fig. 68. Specimens C and D 68

Fig. 69. Pocket size for VAISALA sensor in specimen C 69

Fig. 70. a) PVC tube filled with water and blocked with a latex cork in the bottom; b) Latex cork cup 70

Fig. 71. a) 2 pieces of PVC to facilitate the latex pulling out; b) PVC pieces join together before pouring latex 71

Fig. 72. VAISALA case prepared for pouring latex 71

Fig. 73. a) PVC tube with the additional piece filled with latex; b) 24 hours after the latex was poured the additional piece is removed; c) The latex plug was easily removed pulling it from the extreme 72

Fig. 74. Piece of PVC tube prepared for creating the latex cork in the sensor 73

Fig. 75. Procedure for placing the sensor with the plug at the desired depth: a) Measure the PVC tube; b) Measure the desired depth in the sensor´s wire according to the

pocket size and mark it; c) Insert the sensor in the PVB tube until the mark in the wire is in the edge of the PVC tube 74

Fig. 76. Sensor and latex plug placed in the PVC tube..... 74

Fig. 77. Formwork for the specimens 75

Fig. 78. Guide of the Specimens faces by number 76

Fig. 79. PVC tubes with Gore-Tex placed in the formwork 76

Fig. 80. Concrete specimen covered with plastic to avoid moisture transfer..... 78

Fig. 81. Illustration for the gravimetric test..... 80

Fig. 82. a) Concrete slice after dry hit; b) The sawing should be 2 cm 81

Fig. 83. a) RH readings of different pocket size in specimen A - Honeywell sensors; b) RH readings of different pocket size in specimen B - Sensirion sensors..... 82

Fig. 84. a) RH readings of different type of Gore-Tex in specimen A - Honeywell sensors; b) RH readings of different type of Gore-Tex in specimen B - Sensirion sensors.... 84

Fig. 85. RH readings at different depths for specimen D..... 86

Fig. 86. Moisture loss tendency for the gravimetric test..... 88

Fig. 87. Three months RH readings for the specimen with the concrete used in Paradela DAM 89

INDEX OF TABLES

Table 1. Salt solutions and expected relative humidity in the VAISALA´s calibrator 36

Table 2. Proportions for the salt solutions used in the containers (different salts)..... 37

Table 3. Proportions for the NaCl solutions used in the containers 38

Table 4. Sensors used for each container with different salts 39

Table 5. Sensors used for each container with the NaCl salt 40

Table 6. Glass of water content for each container 41

Table 7. Specimen´s dimensions 66

Table 8. Pocket size for specimen A..... 67

Table 9. Pocket size for specimen B 67

Table 10. Sensors and variables summary for Specimens A, B, C and D 69

Table 11. Concrete mix..... 77

Table 12. Concrete volume for specimens A, B, C and D 77

Table 13. Aggregates correction..... 77

Table 14. Water content for the gravimetric test..... 87

1 INTRODUCTION

Concrete is mainly composed by graded fine and coarse aggregates, sand, cement, water and pores. Water in concrete may exist as chemically bounded, which is the water that has reacted with the cement particles during hydration reactions; and physically bounded, that is the water that did not react with cement and thus occupies the pores. Water inside the pores may either be in the state of vapour, be adsorbed on pore walls, or exist as free water in the liquid state. These distinct states of physically bound water can be removed from concrete by exposure to the environment, or by oven-drying of concrete at temperatures above 105°C. The rest of the water remains chemically bounded.

To measure the internal moisture distribution in concrete it is necessary to determine the moisture at several depths in a concrete specimen at the same time. Continuous measurements of the moisture content at these points give an understanding of the moisture loss in concrete. To achieve this goal, there are several methods that will be explained in this document, but the one to be mainly analyzed is the one that represents the moisture content at a specific depth as the relative humidity of an artificially created macro-pore inside concrete at the same depth.

Comparative behaviour of RH sensors will be addressed under several constant relative humidity conditions. One of the limitations is that RH sensors cannot be in contact with water or a saturated environment; as such situation would cause damage. To be able to embed the sensors inside fresh concrete, a protection method has to be used. For this research work, the sensors will be protected with PVC tube with an interface within the concrete and the sensor of a material that allows the water vapour to pass through but not the liquid water. Gore-Tex® was the adopted material, since it has the necessary properties to assure the mentioned performance requirement.

However, embedding the sensors in fresh concrete with the help of additional materials, make many variables to be analyzed in the study. They can be difference within the pocket size when placing the RH sensors in PVC tubes covered with a Gore-Tex interface, the influence of different types of Gore-Tex, difference with the RH readings when using these materials compared with direct measurements without any cover; and the alternative options for the RH sensor´s protection.

After the way of embedding the sensors is solved, the other task is to create controlled environmental conditions to develop constant RH conditions in order to represent the variables to be analysed in the concrete specimens in an accurate way without being affected by unknown moisture in the environment. To do this, the use of salts to create artificial environments with constant relative humidity was explored. Different salt solutions in different proportions were used to create a desired relative humidity in containers, in a range from 11 % to 97%.

2 METHODS TO MEASURE MOISTURE IN CONCRETE

As stated before, water in concrete is presented as free water held by capillarity, as absorbed water held by surfaces forces and as bound water held chemically. The ideal method of moisture measurement should quantify amounts of these states but this is a difficult task because moisture in concrete is not uniformly distributed, and moisture distribution varies with the exposure time (Li Chunqiu 2008).

To determine moisture profiles in concrete is necessary to measure its evaporable water or water physically bounded. The moisture can be regarded in the following two main categories in concrete: as concentration (mass per volume) and as pore relative humidity. Both categories are related by moisture isotherms.

The pore relative humidity is related to the concrete psychrometric properties as relative humidity is a psychrometric property itself. It is important then to mention both concepts: Psychrometry is the study of gas mixtures including a condensable gas. It is the field concerned with the study of physical and thermodynamic properties of gas-vapour mixtures (Gatley 2005). Psychrometrics or psychrometry or Hygrometry are terms used to describe the determination of these properties (Herrmann S. 2009). Any instrument that can measure the humidity or psychrometric state of air is a hygrometer. The indication sensors used on the instruments respond to different moisture property contents (Kharagpur 2002). Relative humidity is a term used to describe the amount of water vapour in a mixture of air and water vapour (Devres 1994). It is defined as the ratio of the partial pressure of water vapour in the air-water mixture to the saturated vapour pressure of water at those conditions. The relative humidity of air depends not only on temperature but also on pressure of the system of interest (Kuehn 1998). Relative humidity is often used instead of absolute humidity in situations

where the rate of water evaporation is important, as it takes into account the variation in saturated vapour pressure. It is normally expressed as a percentage and is calculated by using the following equation:

$$\phi = \frac{e_w}{e^*_w} \times 100\% \tag{1}$$

where (ϕ) is the relative humidity of an air-water mixture, (e_w) the ratio of the partial pressure of water vapour (H2O) and (e^*_w) the saturated vapour pressure of water at a prescribed temperature (Devres 1994).

The concrete pore structure influences its physical properties, particularly in terms of permeability and strength. Regarding the permeability, the pore network should also be considered. The pore network can be measured by mercury intrusion porosimetry (MIP), but this technique cannot indicate the pore shape or the position of the pores, which are important information to analyze the pore connectivity. On this regard, Kurumisawa et al. (Kurumisawa and Tanaka 2006) developed a technique for the visualization of the pore structure. In this technique the mercury is substituted for gallium. Gallium intruded into the pores is observed in the solid phase by electron probe micro analysis (EPMA). Several observations by EPMA were performed and three-dimensional images of the pore structure were reconstructed by stacking the acquired images of the pore structure. This experiment technique was done to clarify the relationship between water permeability and pore connectivity (Kurumisawa and Tanaka 2006).

Fig. 1 shows a 3D image of a pore structure in a hardened cement paste. In this colour representation, red indicates a high concentration of gallium, while blue means zones of reduced percentage of gallium. Hence, the pixels in blue show the solid phase. The highest concentration of gallium represents a pore of $1\mu m^2$.

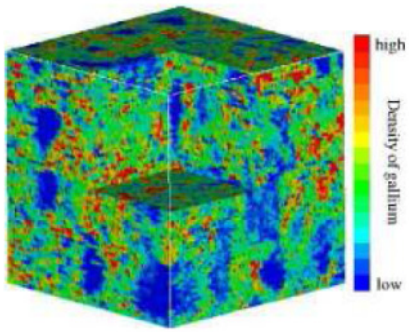


Fig. 1. 3D image of pore structure (Kurumisawa and Tanaka 2006)

The porosity is related with the w/c ratio. The lower is w/c ratio the smaller is the porosity, which means lower pore connectivity as well. The loose of moisture is related with the pore structure trough the permeability, which increases with the porosity. The higher is the porosity, the easier and faster is the water transfer within the concrete and from the concrete to the environment (Baroghel-Bouny 1999; Kurumisawa and Tanaka 2006).

As already indicated, the pore structure can be related with the moisture properties through water vapour desorption and absorption isotherms (WVSI). In this context, various methods can be used namely: the flow division method where dry and saturated air is mixed, the method altering temperature, pressure or both, the volumetric method that isothermally changes the vapour pressure in a vacuum system, gravimetric methods that consist in weighing samples at different relative humidity, and the saturated salt solution method that belongs to the gravimetric type (Baroghel-Bouny 2007).

Desorption and adsorption correspond to the loss of water by drying a specimen (desorption) and to the gain of water exposing the specimen in a humid environment (adsorption). The experiment to determine isotherms consists in enclosing thin specimens of hardened concrete and cement pastes in sealed desiccators. The relative humidity is kept constant in the desiccators by means of saturated salt solution. The specimens are submitted to step by step desorption and subsequent adsorption process while changing the relative humidity using different saturated salt solutions. The mass water content of the specimens is determined by weighing. After removing the small upper stopper of the desiccators, each specimen is hung inside the desiccators from the bottom hock of the electronic balance. The relative humidity is

changed when the moisture equilibrium is reached. The mass water content of the material at the test temperature can thus be plotted vs. relative humidity (see Fig. 2).

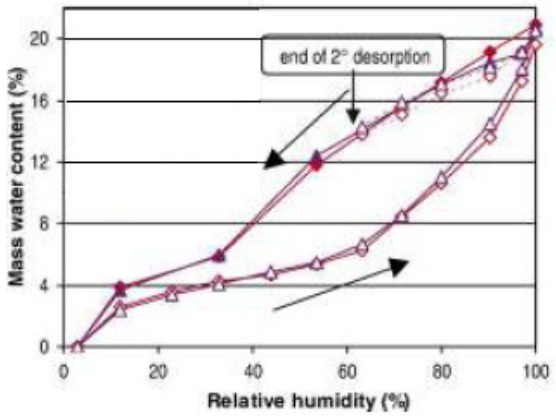


Fig. 2. Water vapour desorption and adsorption isotherms measured at 23°C (Baroghel-Bouny 2007)

The hysteretic behaviour is observed in the desorption-adsorption cycle. Each obtained isotherm depends of the concrete mix (material) and the temperature.

After the pore structure and its relation with the moisture content has been explained as well as the concept of relative humidity, the determination of the moisture profile in its mentioned two categories (as concentration and as pore relative humidity) can be approached. The following methods show some techniques developed by different authors of how to monitor the moisture content in concrete.

2.1 Methods based on concentration

2.1.1 Gravimetric determination

Gravimetric methods consist on determining water content through weighting samples upon oven drying; encompassing absorbed and chemically bound water (DeAngelis 2007). There are automatic moisture analyzers that utilize infrared lamps as a heat source as well. This technique measures the weight loss of hardened concrete slices or specific portions, by comparing the final weight after oven drying to the initial weight before testing. The results may be expressed by weight (weight units according to the measuring system) as the difference of the mass of water present to the dry weight of the concrete sample or by volume (volume units according to the measuring system) as difference of the volume of water to the total volume of the concrete sample (DeAngelis 2007). This method is considered to be the most direct and reliable procedure despite the large number of necessary specimens, since different samples must be used for each measure, and only the average water content of each portion or slice can be obtained (Selih 1996).

H. Akita *et al*, (1996) proposed the analysis of prismatic concrete specimens in order to quantify the moisture transfer experimentally and numerically. Variations in water content were measured at different depths by splitting the specimens and comparing the mass of each piece before and after oven drying at 105°C.

In Akita´s experiment, the specimens were prepared using normal Portland cement, river aggregate (maximum size 20mm) and river sand, with a size of 10x10x40 cm and notched in preparation for splitting as shown in Fig. 3. The specimens were cured for 28 days and after that, the environmental conditions were maintained at a constant temperature of 20°C and relative humidity of 60%.

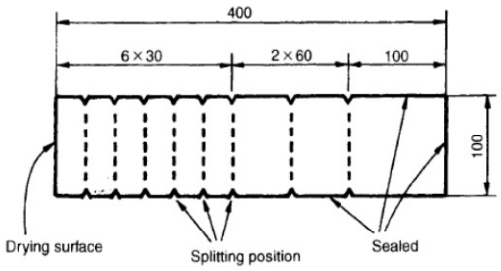


Fig. 3. Dimension (mm) of specimens subjected to one-face drying (Akita 1996)

Four experiments were performed. In the first experiment, a one-face drying (drying surface shown in Fig. 3) was performed in order to observe the water content profiles relative to one direction moisture transfer. The second experiment also involved one-face drying in order to observe the decrease in mass of specimens and to evaluate the surface factors related to water diffusion for different concrete mix proportions, such as water/cement ratio, mass decrease and mass of water. The third experiment involved six-face drying (non sealed specimen) in order to observe the decrease in mass of the specimens as well, but in a wide range of mix proportions and finally, the fourth experiment has the purpose to measure the equilibrium water content at various levels of atmospheric humidity, which means measure the water content when the specimen gets its equilibrium with the environmental RH (Akita 1996).

Fig. 4 shows the experimental and the calculated relative water content profiles for one-face drying of a specific concrete mix with a water/cement ratio of 50% and 43% of sand content. The dispersion probably occurs because each split piece has a different thickness and coarse aggregate ratio (Akita 1996).

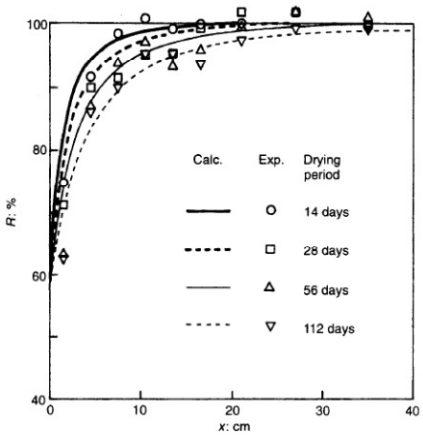


Fig. 4. Profiles of relative water content for one-face drying, where X represent the specimen depth in cm (Akita 1996)

J. Selih (1996), used a modified gravimetric method to obtain the local moisture content regarding the redistribution of moisture after sealing the drying surface. On his experimental program, measurements of moisture content were performed on normal and lightweight concrete cylinders with length of 100mm, 150mm and 200mm, and diameter of 100mm. The studied concretes had the following composition: water/cement ratio of 40% and 60% (normal Portland cement), 34% of coarse aggregates, and 31% and 36% of fine aggregates of the fresh concrete volume. The maximum size of the coarse aggregate is 12.5mm.

The cylinders were cast into plastic moulds and covered with a plastic sheet for 12 hours to prevent water evaporation from unhardened concrete. After this, the cylinders were placed in the moist curing room with relative humidity within 95% to 100%. Moist curing time varied from 0 to 28 days, and when the pre-specified moist curing period has elapsed, the cylinders were exposed to drying on the top surface at constant temperature of 22 ± 1°C and relative humidity of 50 ± 5%. Zero days moist concrete (specimens which were not cured) was exposed to drying immediately after removing the plastic sheet. Then cylinders were placed vertically with the drying surface on the top. The moulds were not removed during drying neither during moist curing. On this way, the side and surface of the specimens were sealed against the moisture flow, letting the moisture flow be unidirectional along the longitudinal axis of the cylinder as shown in Fig. 5. The test was conducted for drying periods of 0, 1, 3, 7, 28 and 90 days.

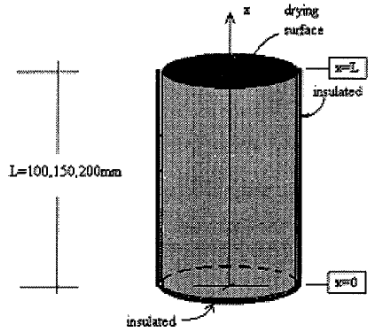


Fig. 5. Cylinder with unidirectional moisture flow (Selih 1996)

Local moisture measurements were made by splitting the cylinders into discs each with 25 mm thick. To facilitate the saw cutting process, thin PVC meshes are placed during casting into each cylinder perpendicular to its axis at equal distances of 25mm, in order to form splitting planes, as shown in Fig. 6 (Selih 1996).

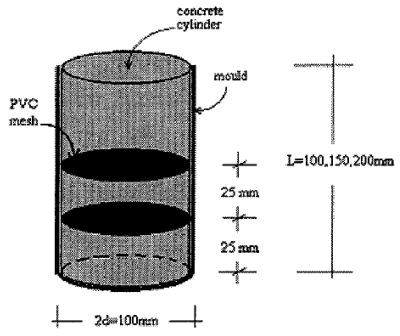


Fig. 6. Schematic representation of the cylinder tested with the PVC meshes (Selih 1994)

The PVC meshes may affect water movement in the material if the change of the structure occurs due to segregation of coarse aggregate, since a thin layer of bulk cement paste can be formed adjacent to the mesh (Selih 1994).

After splitting the cylinder, each 25mm disc was weighed, then dried at 95°C in the oven for 3 days, and re-weighed. The amount of moisture in a disc was taken as the difference between

the wet and the dry weight, and represent the local moisture content of the cylinder (Selih 1996).

Fig. 7 shows the experimental and numerical results of the tests according to the drying period. In general, it can be observed that rapid changes of moisture content and consequent large drying rates occur during the first days of drying. The shape of moisture profile starts changing between 3 and 7 days, when increased moisture content gradients have taken place near the drying surface. The drying rates decrease indicate that capillary flow of free liquid water is no longer present in the porous medium, and water moves due to the concentration variation (Selih 1996).

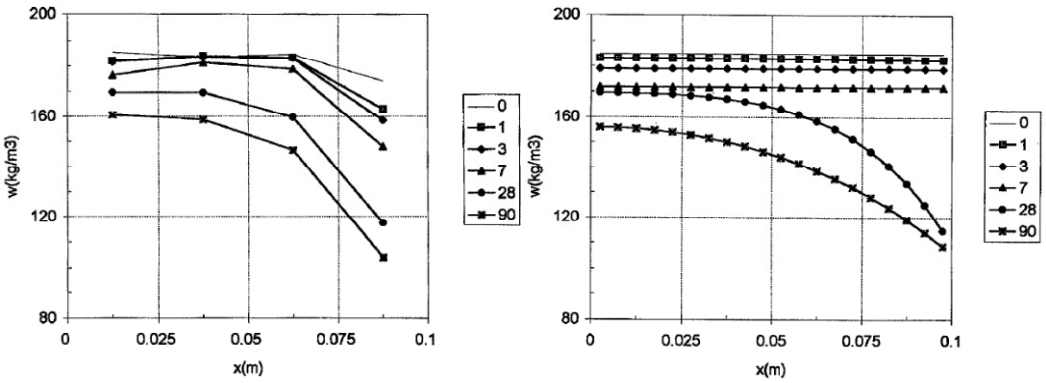


Fig. 7. Moisture content distribution through the depth in the cylinder (a) Experimental results, (b) numerical results; 1 days moist cured lightweight concrete with water/cement ratio of 0.4, at dry period of 0, 1, 3, 7, 28 and 90 days (Selih 1996)

In the work of Amba *et al.* (2010) the effect of drying on the structuring of cement based materials was studied, as well as its consequences on the development of length changes. They determined water gradients on these materials through a gravimetric method designated as “Slice Test”. The moisture content in the material thickness was quantified with this method by heating in the oven at 105°C for the free water and 550°C for the bound water in a cement based material.

Two mortars were studied with the same water/cement ratio (MA, MB), with and without vinyl polymer powder respectively (used to reduce porosity in the mortar). The samples had dimensions of 40x40x160mm and were kept in a laboratory with a controlled temperature of 20 ± 1°C and a relative humidity of 65 ± 5% (J.C. Amba 2010).

For each mixture, the moisture loss was measured by drying each mortar specimen (MA, MB) from one exposed surface only. The prisms were cast immediately and the drying process was allowed through their top surface (Fig. 8). At an age of 24 h the specimens were demoulded. The top surface of one specimen was left free to dry, while the others five were sealed using an adhesive aluminum foil to prevent drying. The mortar slices are taken by sawing along a direction parallel to the drying surface. The slices were 5 mm thick. Measurements were made at depth of 3mm, 10mm, 17mm, 25mm, 32mm and 38mm from the drying surface (see Fig. 8).

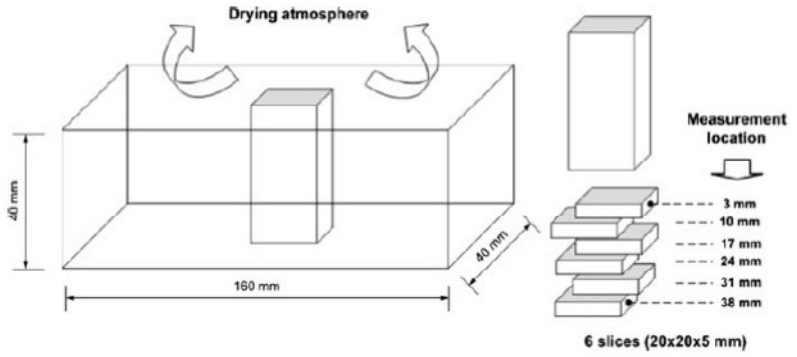


Fig. 8. Sampling and geometry details of hardened mortar slices (J.C. Amba 2010)

The technique consisted in measuring the weight loss of hardened mortar slices upon heating at 105°C and 550°C. The water loss up to 105°C is assumed to be free water (contained in the pores) and that between 105°C and 550°C is bound water.

Fig. 9 shows the results of the free and bound water profile for different depths inside concrete for the samples exposed to dry at 3, 7 and 28 days.

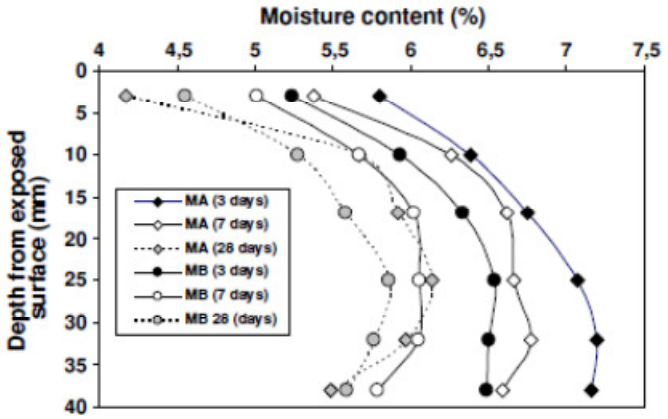


Fig. 9. Profiles of free water for mixes MA and MB (J.C. Amba 2010)

The amount of free water in each sample decreases through time. The decrease of free water content as shown in Fig. 9 is linked for a large part to the drying of mortar and for a minor part to its consumption during the cement hydration process. In the case of thin mortar layers the effect of drying is more harmful than in massive structures. The increase in bound water is related to the fact that concrete will always absorb water along the time (J.C. Amba 2010).

The procedures used by Akita, Selih and Amba to determine the moisture profile by a gravimetric method explained above are similar to each other with slight differences in specimen sizes.

2.1.2 Gamma – Densitometry

The gamma densitometry is a nondestructive testing method commonly used to control the density of civil engineering materials (Villain and Thiery 2006).

With the aim of increasing the knowledge on the effect of water in the Alkali-Silica reaction S. Multon *et al*. (2004) executed real scale experiments in two 3m long beams of 0.25x0.5 m^2 cross section in which they measured the water content and the moisture gradient during two years period. The beams were stored in a large climatic-controlled room at 38°C and 30% RH. The beams were submitted to a moisture gradient created by immersing the bottom faces in water and exposing the upper faces to the ambient at 30% RH. The lateral faces are covered by three sheets of watertight aluminum on the upper 430 mm and placed in contact with water

on the lower 70 mm (see Fig. 10). These moisture conditions lead to drying in the upper part, resulting an unidirectional moisture gradient over the upper 430mm of the beam (S. Multon 2004).

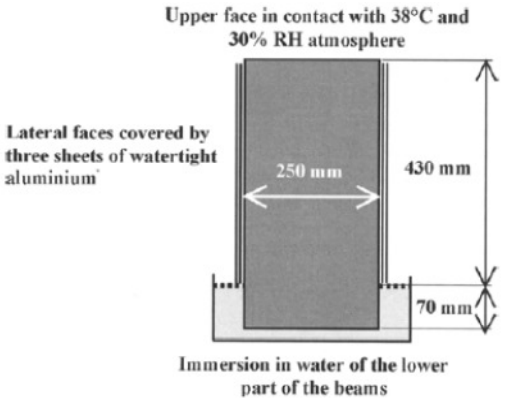


Fig. 10. Moisture-controlled environment of the beams (S. Multon 2004)

The principle of this method is based on a beam of gamma rays emitted by radioactive source and passing through the concrete (see Fig. 11). The relative intensity of the transmitted particles is related to the mass of the traversed material m_c, the mass variation of the traversed points can thus be measured. Since chemical evolutions do not lead to significant losses of mass, the mass variation in these beams stem solely from water evaporation; and can be interpreted as the profile of water content variations (S. Multon 2004).

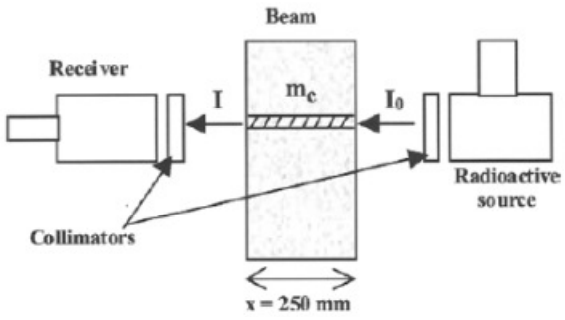


Fig. 11. Principle of the gammadensitometry technique (S. Multon 2004)

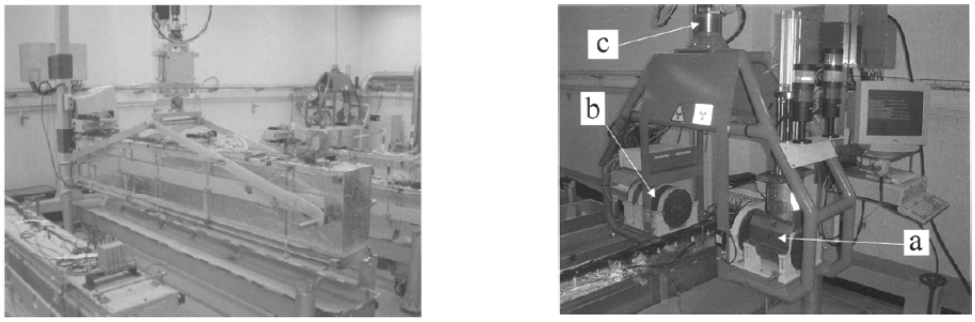
The gammadensitometry is based on absorption of the gamma ray emitted by a radioactive source of Cesium Cs^{137} (Villain and Thiery 2006). The relation between intensity I of the flow of transmitted particles and traversed mass m_c is as follows is based on the Lambert´s Law (S. Multon 2004):

$$I = I_o.\exp(-\mu'.m_c) \quad (2)$$

where I, and I_o are the intensities of the transmitted and of the emitted flow, μ' is the coefficient of mass absorption of the concrete and m_c the mass traversed by the gamma ray beam.

The mass variation of the volume intercepted by the gamma ray can be measured at different depths, so water content variation along the height of the concrete beam´s cross section can be monitored. The calculation method assumes that at each measurement the flow intercepts the same volume of material (S. Multon 2004).

Fig. 12 shows the experimental set up for the test, where it is visible the concrete specimen partially immersed in water and then the radioactive source for the gamma ray with the rest of the equipment.



a) b)

Fig. 12. a) Real scale concrete beam b) Gammadensitometry equipment (a: receptacle of the radioactive source, b: receiver for measuring emitted and transmitted flows, c: electric jack connection) (S. Multon 2004)

The measurements of emitted and transmitted flows were recorded on the computer and mass variations were calculated. The result is a mean drying profile for each beam and for each measurement (S. Multon 2004).

Since the beams deform and high-quality positioning for the radioactive source is required, it is quite difficult to use a fixed reference in the beam. Regarding this, the positioning has been based on the use of a laser-receiving diode couple and three marks placed on the beam (see Fig. 13)

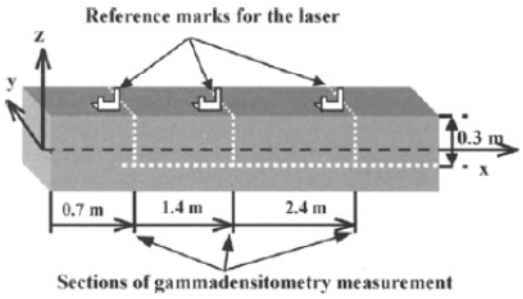


Fig. 13. Location of the gammadensitometry sections on a beam and reference marks (S. Multon 2004)

A reference mark consists of a metal plane with three edges (two vertical and one horizontal). An optical control allows a laser to recognize the edges. Depending on whether, or not, the diode receives the laser signal, an automatic device give reference of its position along both directions. Then, positions the gammadensitometry equipment with respect to the three measured sections are obtained (S. Multon 2004).

In the next sentences a brief explanation of the gammadensitometry measurement accuracy and data processing is presented.

The mean drying profile consists in calculating the relative variation in mass being traversed by the gamma flow, which is obtained by the following equation (S. Multon 2004):

$$(\%)\frac{\Delta mc}{mc} = \frac{mc2 - mc1}{mc1} x100 \quad (3)$$

where $mc1$ and $mc2$ are the masses traversed at different times (1 and 2) and mc is the mean measurement value of the three sections at each height. The mean value accuracy is 0.4% in terms of the mass variation. The gammadensitometry equipment has allowed to measure the mass variations in 5 levels for 3 vertical sections (15 points) along the upper 300 mm of the beams (S. Multon 2004).

Fig. 14 shows the results of the measurements to obtain the drying profile related with the relative mass variation for the upper 300 mm from 5 up to 430 days.

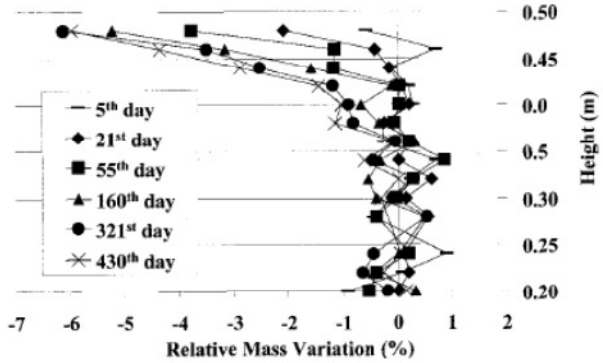


Fig. 14. Relative mass variation along the upper 300 mm of the beam (S. Multon 2004)

Gammadensitometry method is also used to determine drying and carbonation profiles, as Géraldine Villain et al. (2006) have shown in one of their experiments using this technology. The set up they used is shown in Fig. 15, which consists of a concrete cylindrical sample of 100 mm high that is tested at different depths through the gamma ray beam, by moving it in the vertically direction by a robot.

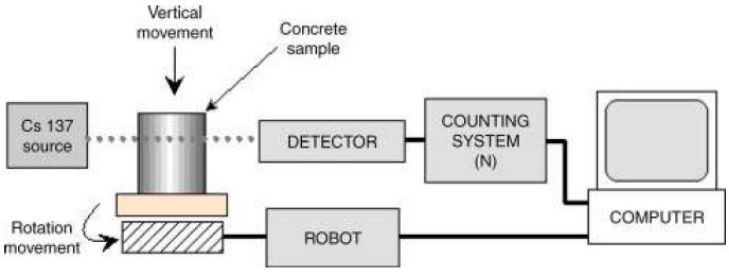


Fig. 15. Gamma-ray measurement set-up (Villain and Thiery 2006)

The drying profile of the sample after 1 month of drying at 45°C expressed in density is showed in Fig. 16. As expected, the lowest density is presented in the upper and lower surface of the sample.

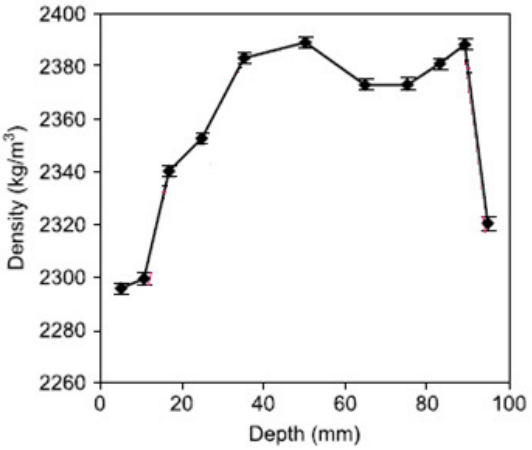


Fig. 16. Density measured after 1 month of drying (Villain and Thiery 2006)

2.2 Methods based on relative humidity

2.2.1 Relative humidity measurements embedding sensors in concrete

2.2.1.1 Relative humidity sensors

There are two main types of relative humidity sensors, capacitive and resistive. The capacitive sensor consists of a thin layer of water absorbent polymeric or inorganic material that is coated onto a conductive base. This layer is then covered with porous conductive layer material. With the increase of the relative humidity, the water content of the sensing element increases too (Wiederhold 1997) . Water has a high dielectric constant, which means that the combination of two electrodes with the water between can store a relatively high electric charge. This electrical capacity is measured by applying rapidly reversing (AC) voltage across the electrodes and measuring the current that passes. The polymer or inorganic material is

usually aluminum oxide and just plays an indirect part of the measurement. An example of a sensor of this type, with dimensions 7 x 4 x 0.5 mm can be seen in Fig. 17.

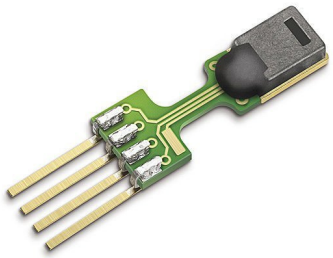


Fig. 17. Capacitive sensor (www.sensirion.com 2009)

The change of capacitance of these capacitive sensors is, however, small when even compared with the capacitance of few meters of cable. This means that the electronic process of data acquisition has to be completed close to the sensor. If one data logger is connected to several relative humidity sensors, each sensor will need its own power supply and relatively bulky electronics(www.conservationphysics.org 2010).

The resistive relative humidity sensor consists of a thin wafer of absorbent polymer, printed with two interlocking combs of conducting metal or carbon. The electrical resistance across the surface of the polymer is measured, being dependent on the changes of water content. This sensor also needs an alternating excitation voltage to avoid burning it by causing one-way electrolytic ion movement in the polymer, which is a process that can generates a big amount of heat energy, higher than what the sensor internal resistance can take (see Fig. 18).

These sensors have a relatively slow response to relative humidity changes. Therefore, their use and application has been mostly relegated to building environment related research (www.conservationphysics.org 2010).

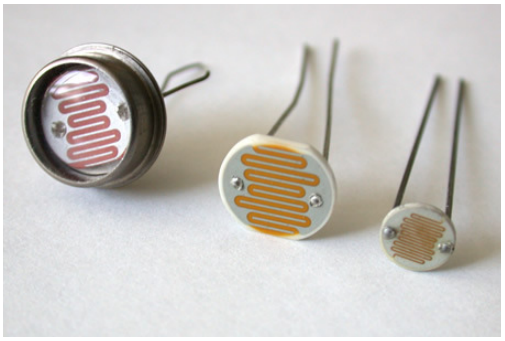


Fig. 18. Resistivity Sensors (www.conservationphysics.org 2010)

However this type of sensors requires data loggers capable of providing the pulsed excitation. These sensors are commonly used in places with a stable environment, since they are relatively delicate (www.conservationphysics.org 2010).

In fact, relative humidity sensors are easily contaminated by water soluble salts. The sensor can be protected with Gore-Tex or with a thin layer of silicone (less than 0.5 mm). These materials allow the water molecules to flow and offer resistance to ions penetration that can influence the behavior of the sensor. However, the envelope formed by this thin layer should not touch the sensor surface. These kinds of semi-permeable membranes will lengthen the time response for changes in relative humidity of the thin film sensors from about a minute to twenty minutes. Due to these reasons, this type of sensor is seldom used (www.conservationphysics.org 2010).

Another type of RH sensors is the Nanotechnology/Microelectromechanical system sensors. Cutting edge nanotechnology/MEMS, which have matured in recent years, represent and innovative solution to current monitoring systems, leading to wireless, inexpensive, durable, compact, and high-density information collection, processing and storage devices for structural health monitoring (Norris, Saafi et al. 2008).

MEMS devices are being manufactured using the same materials and process as microelectronic devices such as microprocessors and memory chips. These manufacturing methods permit the devices to be small and inexpensive enough to be distributed throughout a structure in numbers from hundreds to millions. The common manufacturing process also

permits the integration of mechanical actuators with electronics for control, processing and communication. This combination introduces the ability to direct sense and interact with the structural environment (Norris, Saafi et al. 2008).

There are several advantages of a MEMS-based monitoring system over other methods of condition assessment and monitoring. MEMS devices can be embedded, bringing their readings closer to the true in situ properties of the structure and not estimative based on external visual inspections or expensive non destructive tests. MEMS technology has the potential to measure the properties of interest directly. They are small and encapsulated, which make them difficult to damage (see Fig. 19) while wireless technologies make them easy to embed (Norris, Saafi et al. 2008) .

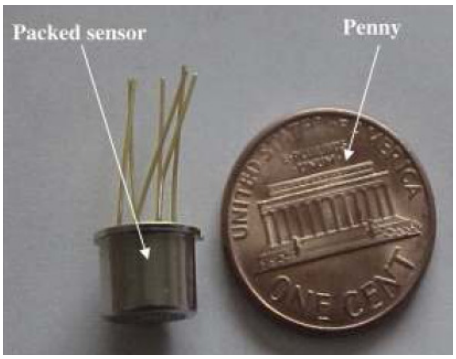


Fig. 19. Packaged MEMS sensors (Norris, Saafi et al. 2008)

A preliminary evaluation of embedded MEMS sensor response was made to evaluate the feasibility of embedding this sensor to measure relative humidity and temperature in a specific depth in a concrete specimen. Five concrete cylinders of 152 mm (diameter) x 305 mm (length) with a water-cement ratio of 0.55 were tested. For each specimen a MEMS sensor was embedded at the middle depth of the specimens in a cured room at 22° C and 50% RH. A data acquisition system was used to power the embedded device and monitor the moisture temperature trough electrical cables (Norris, Saafi et al. 2008).

Fig. 20 shows the typical voltage outputs of the embedded sensor during the 24 hours of curing. The temperature output voltage increased to its maximum of 1.23 V after 12 hours of curing at room temperature and decreased slowly. This maximum voltage corresponds to the

peak of the maximum temperature generated by the hydrated cement paste. The relative humidity output voltage reached its maximum upon embedment of the sensor in fresh concrete, and this maximum voltage, 0.026 mV, corresponds to a relative humidity of 100% which indicated saturation of the sensor (Norris, Saafi et al. 2008).

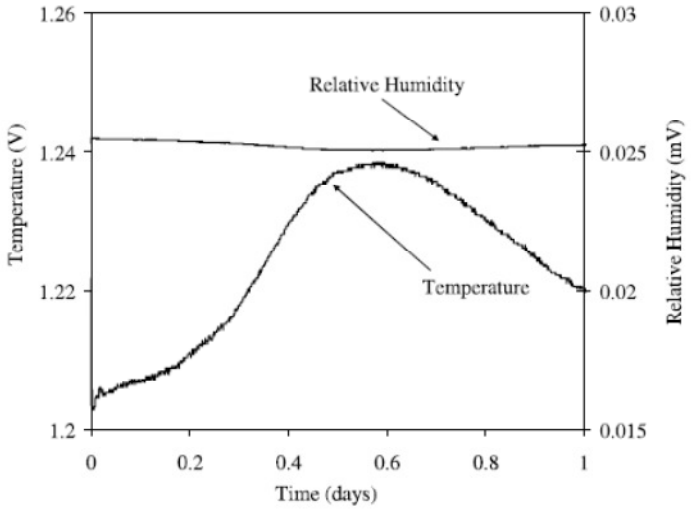


Fig. 20. MEMS response after 24h of curing (Norris, Saafi et al. 2008)

The decrease in the humidity voltage at early ages while the specimens are still in plastic moulds is mainly attributed to self-desiccation, where the use of water by the hydration process reduced the moisture content (Norris, Saafi et al. 2008; Seungwook Lim 2009).

After the specimens were removed and exposed to ambient air, the relative humidity voltage decreased significantly due to moisture diffusion as shown in Fig. 21.

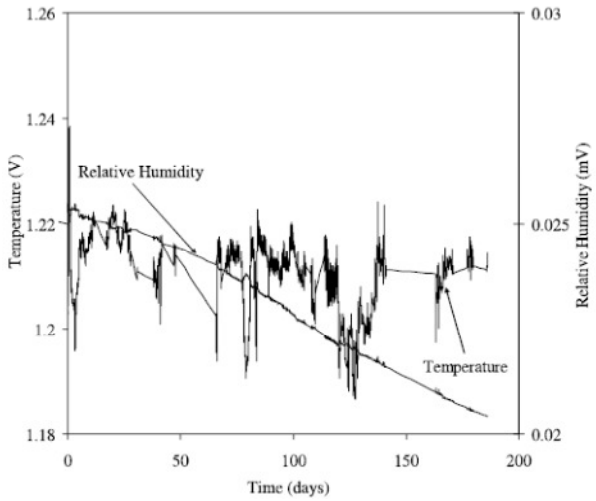
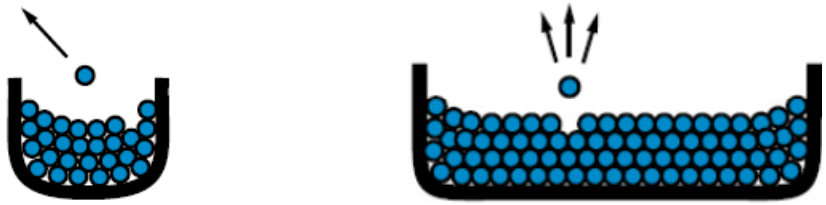


Fig. 21. MEMS response after 200 days of curing (Norris, Saafi et al. 2008)

2.2.1.2 Techniques for relative humidity measurements inside concrete

As explained in previous chapters, relative humidity in concrete is a property of the air adjacent to liquid water held in the pores. Within each pore, the interface between the liquid water and the air forms a meniscus. The restraining forces to hold the water molecules inside the meniscus are dependent of its curvature, the evaporation rate and the local relative humidity in the pore. Fig. 22 shows how water molecules require higher or lower energy to escape depending of the possible directions they have to escape depending of the curvature of the meniscus, being higher in convex shape (Fig. 22a) and lower in flat shapes (Fig. 22b) according to the surface tension (Zachary Grasley 2006).



(a) (b)

Fig. 22. Meniscus shape related with the escape of the water molecules (a) convex, (b) flat (Zachary Grasley 2006)

It is important to note that relative humidity is not a direct measure of the moisture content. In fact, the relative humidity is a measure of the concentration of water vapor in concrete, while the moisture content is referred to the mass of water in the specimen. Thus, moisture flow in concrete may be calculated by measuring variations in relative humidity during the drying process through the thickness of a concrete specimen (Zachary Grasley 2006).

Using capacitive sensors, Z. Grasley *et al*. (2006) measured the relative humidity, at an age of 1 day, in concrete specimens with water/cement ratio 0.44 after two sides of the specimens have been exposed to 50% RH ambient conditions. Although capacitive sensors can have reduced accuracy at relative humidity values exceeding 90%, they typically provide better linearity than resistive sensors. To solve the problem of the several hours that capacitive sensors can take to reach equilibrium and provide valid readings; and also the fact that RH sensors cannot be directly exposed to fresh concrete, the sensors are mounted in plastic tubes with Gore-Tex caps and then embedded in fresh concrete. This material protects the sensor from liquid water but allows vapor transmission. The vapor pressure within the airspace around the sensor and in the concrete pores tends to be in equilibrium. The methodology of Grasley *et al.* allowed the sensor to be permanently embedded in the concrete reaching its equilibrium and obtaining valid readings. The readings inside the concrete specimen at different depths from the drying face after 3, 5 and 7 days are shown in the Fig. 23 (Zachary Grasley 2006).

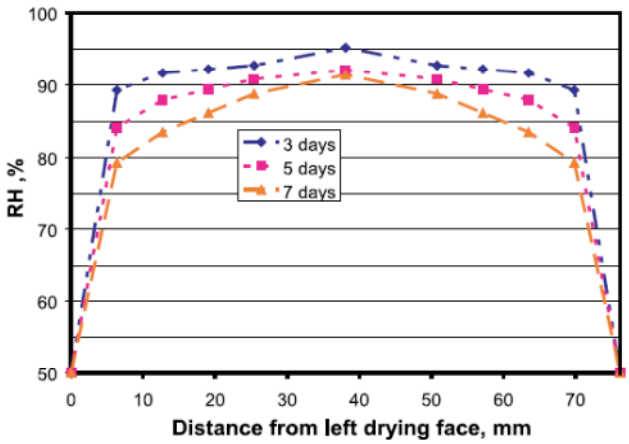
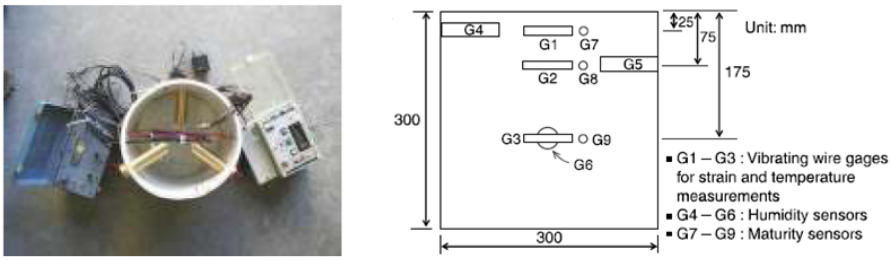


Fig. 23. Evolution of relative humidity in a concrete specimen (Zachary Grasley 2006)

To embed the sensors inside concrete, it is important to make a difference between installing the tubes in the mould before casting (without drilling) and drilling holes into hardened concrete to embed the sensors afterwards, as it has been mentioned in L.J. Parrot document. The drilling process may affect the local water content in the specimen (Parrott 1990).

Seungwook Lim *et al.* (2009) show a proper mould on their work to determine moisture profiles and shrinkage in early age concrete pavements, in a 300 x 300 mm concrete cylinder under uniaxial drying (see Fig. 24).



(a) (b)

Fig. 24. (a)Top view with data acquisition devices (b) Sectional view (Seungwook Lim 2009)

The measurements were taken at three different depths (25, 75 and 175 mm) having started 2.5 hours after casting and continued for 7 days in an environmental chamber under 60°C and 25% RH to accelerate the moisture variation in concrete. The relative humidity had a ± 2% error range. The results are presented in the Fig. 25 (Seungwook Lim 2009).

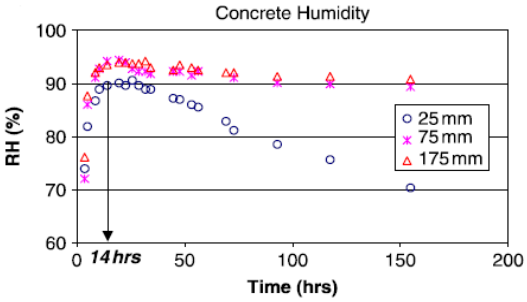


Fig. 25. Relative humidity measurements at 25, 75 and 175 mm of the drying cylinder specimen (Seungwook Lim 2009)

The initial readings show the behavior of the RH sensors when reaching relative humidity values near the saturation stage. For the readings at different depths, the relative humidity value at the point near the drying surface decreases faster than those measured at 75mm and 175mm depths. This shows the effect of drying depth on the concrete humidity, which normally causes the differential shrinkage of concrete (Seungwook Lim 2009).

An alternative method to measure relative humidity is presented by Viggo Jensen (2003), which is called Wooden Stick Method. This method is applicable to concrete with high internal humidity. The concept of the system is based on the use of inexpensive equipment with simple systematic procedures to carry out the measurements (Jensen 2003).

The method consists in measuring the electrical conductivity between two steel needles pressed into a specific wood (Gonystylus macrophyllum due to previous research about its accuracy and performance). This correlates the electrical conductivity with the water content in the wood. The temperature has only a minor influence on the electrical conductivity in the wood, in opposition with the case of concrete (Jensen 2003).

The wooden sticks have to be calibrated. On Viggo Jensen´s experiment the sticks had a diameter of 12 mm and 45 mm long. For each wooden stick, calibration curves of adsorption and desorption were made. The experience shows that calibration curves vary between wooden sticks, so the accuracy of the measurements is improved by the use of individual calibration curves rather than by one standardized curve. Fig. 26 shows an example of adsorption and desorption for one wooden stick and 95% confidence interval calculated from 112 wooden sticks. There is a steeper inclination at higher relative humidity, which means that the sensitivity is improved with higher relative humidity, opposite to the commercial humidity sensors, where measurements in a relative humidity higher than 98% are uncertain very often.

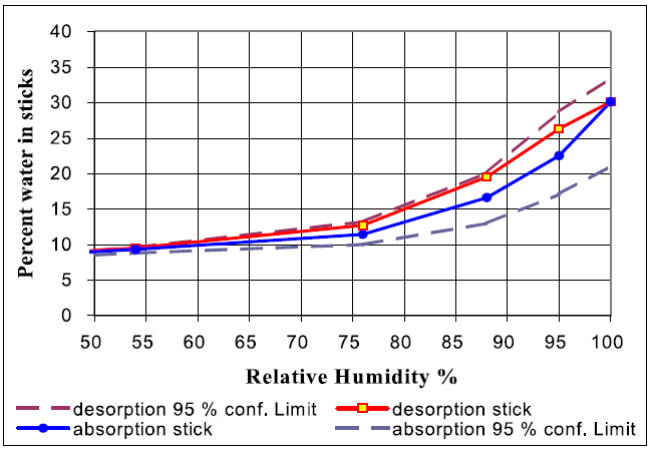


Fig. 26. Calibration curves for wooden stick and the 95% confidence interval for 112 wooden sticks (Jensen 2003)

The wooden stick method was calibrated against commercial methods to assess its reliability. The chosen commercial sensor was AHEAD hygrotemp II with an accuracy of ± 2% RH. Fig. 27, shows the correlation between the relative humidity measurements of the wooden stick and the AHEAD hygrotemp II. Both methods measured similar values of relative humidity (Jensen 2003).

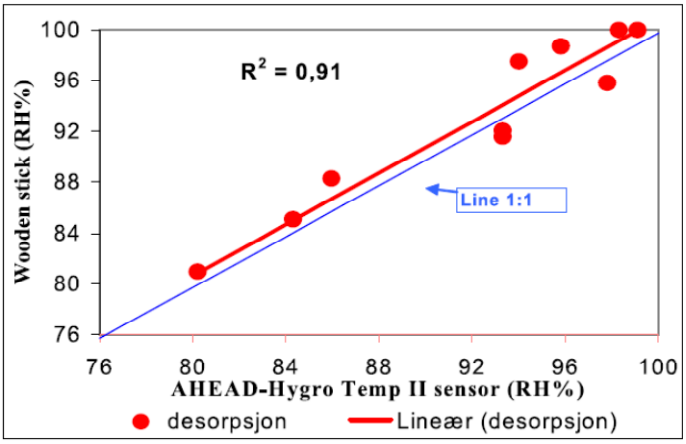


Fig. 27. Correlation between wooden sticks by use of the desorption curve and AHEAD hygrotemp II sensors (Jensen 2003)

In this experiment two wooden sticks (5cm, 25 cm and 40 cm from the surface) were mounted in a specially fabricated plastic tube inside a real structure as shown in Fig. 28. The plastic tube can be modified with only one wooden stick or several more depending on the structural dimensions. The contact within the concrete and plastic tube was assured by epoxy adhesive. Measurements were simple to carry out. The wooden sticks are pulled out from the tube in the concrete and the electrical conductivity is measured and converted in water percent. The relative humidity is estimated from the calibration curve of the stick (Jensen 2003).

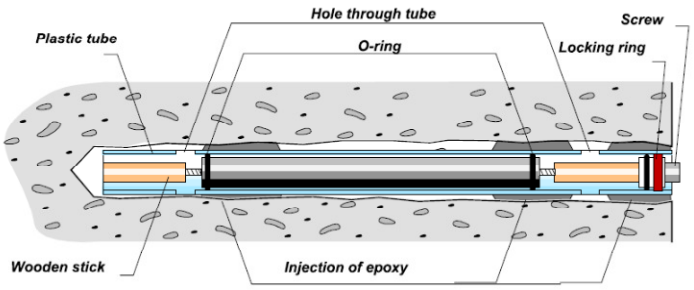
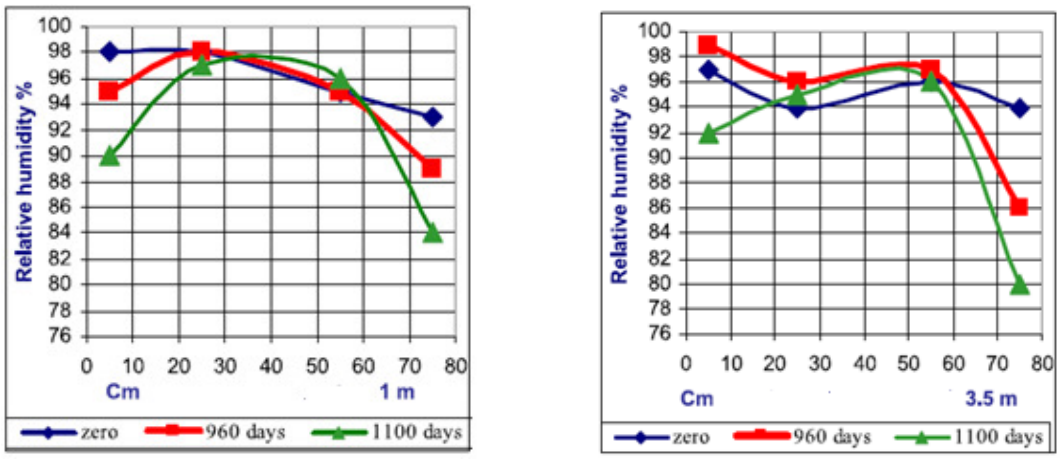


Fig. 28. Plastic tube (diameter 2 cm and length 25 cm) mounted with 2 wooden sticks (Jensen 2003)

The wooden stick method gave valuable information on the long term behavior of the relative humidity in concrete structures. Fig. 29 shows the humidity profiles of a structure where the wooden sticks were placed in different depths and different time of permanency. Results show that the relative humidity is higher in outer surfaces and reduces towards the middle of the elements (Jensen 2003).



(a) (b)

Fig. 29. Humidity profiles of a structure with wooden sticks at (a) 1 m and (b) 3.5 m (Jensen 2003)

2.3 Equipments for RH measurements in the scope of this research

2.3.1 Measuring systems

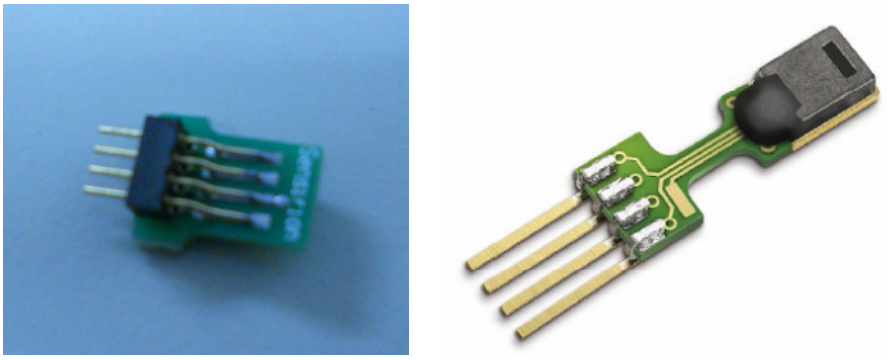
The measurements performed in the scope of this research work carried out with three different brands of sensors: Sensirion, VAISALA and Honeywell. These sensors where chosen as they have a relatively low cost and are commercially available. The shape and size of these sensors allow them to be easily inserted in concrete, which is the chosen procedure to measure relative humidity at different depths.

All these sensors have the same measurement principle, based on capacitance.

2.3.1.1 Sensirion Sensors

The Sensirion sensors SHT21 and SHT71 shown in Fig. 30 were used in this experiment. These sensors are fully calibrated (every sensor is individually calibrated and tested), have

low power consumption, long term stability and digital output, which is measured through the datalogger Sensirion Evaluation Kit EK-H4.



a) b)

Fig. 30. Sensirion sensors a) SHT21 and b) SHT71 (www.sensirion.com 2009)

The accuracy of the SHT21 sensors is ± 3%RH, with a response time of 8 seconds (the time the sensor takes to recognize and read changes in the RH). Regarding the operating conditions, the sensor works stable within the recommended normal range reproduced in Fig. 31. According to the manufacturer, long term exposures to conditions outside the normal range, especially at humidity higher than 90%RH, may temporary offset the RH signal (± 3%RH after 60 hours). After return to normal range, the sensors slowly returns to normal behaviour and response time, according to the Sensirion SHT21 data sheet. A reconditioning procedure may be used to accelerate the elimination of the offset. The procedure is as follows: baking in the oven at 100–105°C and less than 5%RH for 10 hours. Then Re-Hydration at 20–30°C and 75%RH for 12 hours (John Newman 2003).

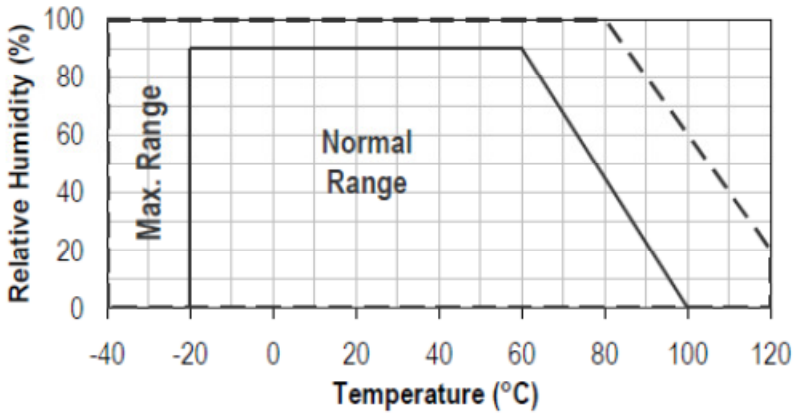


Fig. 31. Operating conditions for the SHT21 sensor

The Sensirion sensor SHT71 has similar characteristics to the SHT21, except for the fact that it has higher accuracy (± 1.8%RH), being more expensive as well. The operating conditions are similar as for SHT21, but the normal range is higher (until 95%RH), as shown in Fig. 32.

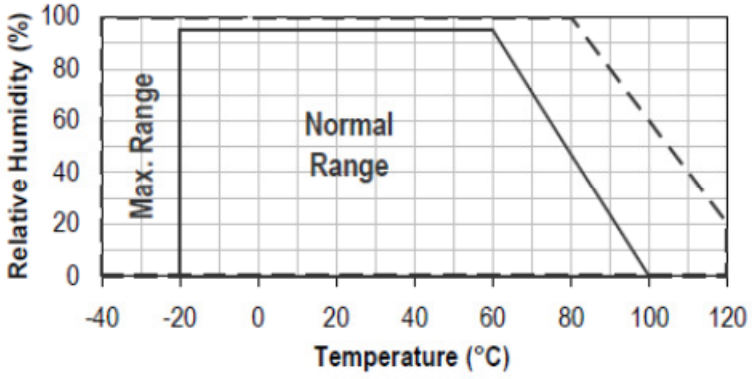


Fig. 32. Operating conditions for the SHT71 sensor

2.3.1.2 Honeywell Sensors

The Honeywell sensors HIH 4000 and HIH4010 have been used on this experiment (see Fig. 33). These sensors have a nearly linear voltage output in regard to moisture variations. The input current is 5V and each individual sensor has a calibration data sheet available.

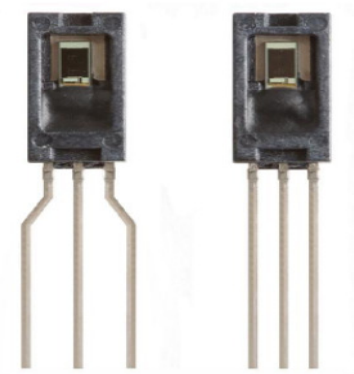


Fig. 33. Honeywell sensors HIH4000 and HIH4010 series 003 and 004 from left to right

The HIH4000 and HIH4010 sensors have an accuracy of ± 3.5% in a humidity range from 0% to 100%. The response time is 15 seconds for the HIH4000 sensor, and 5 seconds in the case of HIH4010. The supply voltage range varies from 4V to 5.8V for HIH4000, and 2V to 5V in the case of HIH4010. The operating temperature range is from -40°C to +85°C.

Data collection from the Honeywell sensors can be made with a general purpose data logger (with capacity to measure potential in V). In the case of this research, a Data Taker DT515 (see Fig. 34) together with a CEM20 expansion module was used (with a total of 30 measuring channels). The interface used for these sensors is called DeLogger which belongs to the Data taker® suite.

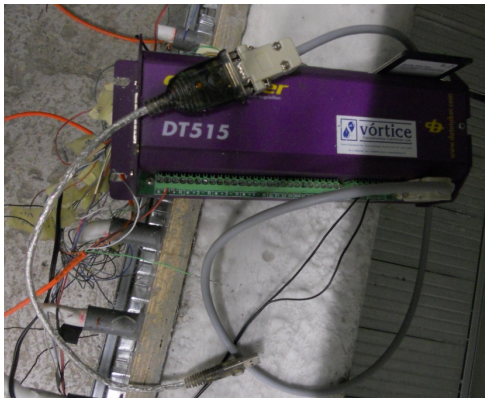


Fig. 34. Data taker DT515 and CEM20 expansion module

2.3.1.3 VAISALA Sensor

The VAISALA sensor HM44 (see Fig. 35) has been designed specially to measure relative humidity inside concrete. This sensor operates with an analogue signal, instead of digital, but the measure principle is the same as Sensirion sensors, which is a capacitive sensor. The measurement range for relative humidity is from 0 to 100% RH, with an accuracy of ± 2% RH for 0 to 90% RH and ± 3% RH for 90 to 100% RH. The response time is 15 seconds, which is lower than in Sensirion sensors.



a)



b)

Fig. 35. a) VAISALA´s HM44 sensor; b) Data logger

3 USE OF SALT SOLUTIONS FOR ASSURING CONSTANT RELATIVE HUMIDITY CONDITIONS IN CONTAINED ENVIRONMENTS

The research purposes of measuring humidity profiles and corresponding shrinkage in concrete, require the testing of a significant number of samples. One of the main issues that influence moisture profiles in concrete samples is related to the environmental conditions to which the specimens are subjected (e.g. humidity, temperature, wind speed). For a proper characterization of the influence of environmental conditions on moisture losses, such conditions have to be known and stable. The experiments initially envisaged in the scope of this project aim to have constant temperature, relative humidity and wind speed throughout the whole testing period.

The experiments described in this chapter have the intention of creating known environmental conditions in containers where the samples and specimens are to be tested. Such conditions are relatively easy to achieve through the use of climatic chambers. However, the number of climatic chambers is usually limited in laboratories, and the available climatic conditions are not always simultaneously suitable for the experiments conducted by the several researchers of the laboratory.

With this limitation in view, it was decided to test the possibility of assuring constant humidity conditions inside plastic containers through the use of salt solutions usually applied in calibration of humidity sensors. The intention is to have several testing humidity inside a climatic chamber that just needs to control temperature (much cheaper than humidity control). In the scope of this report, a walk-in climatic chamber with 20°C ± 0.2°C and RH = 60% ± 3% was used.

To achieve the necessary conditions, salt solutions with a known target relative humidity (according to their use in humidity sensor calibration in VAISALA´s user manual) were placed in closed containers (where specimens will expectably be placed for testing). The humidity inside the containers was continuously monitored through the use of several types of humidity sensors, thus allowing relating the salt solution efficiency in view of the targeted relative humidity in the container, and its stability along time.

Conclusions are withdrawn in regard to the behaviour of the tested types of humidity sensors.

3.1 Sal solutions for humidity calibrators

In the scope of this research, the VAISALA humidity calibrator HMK15 (see Fig. 36) was purchased, together with the VAISALA HM44 set for measuring humidity in concrete.



Fig. 36. VAISALA HMK 15 relative humidity calibrator (www.vaisala.com 2006)

The HMK15 calibrator is based on known relative humidity being assured by salt solutions for a specific chamber volume of 20 cm^3 (diameter = 5 cm, height = 3.5 cm). The salts used in the calibrator are Lithium chloride (LiCl), Magnesium chloride ($MgCl_2$), Sodium chloride (NaCl) and Potassium sulphate (K_2SO_4). The salt solution and the expected relative humidity values in the chamber are shown in Table 1.

Table 1. Salt solutions and expected relative humidity in the VAISALA´s calibrator

Salt	Water content	Expected relative humidity
15g LiCl	12 ml	11%
30g MgCl2	3 ml	33%
20g NaCl	10 ml	75%
30g K2SO4	10 ml	97%

According to these proportions the same salts solutions were poured in the containers, expecting to obtain relative humidity values close to those ones established in VAISALA´s calibrator. The effect of the amount of salt used in each container was also checked.

3.2 Experimental program

3.2.1 Environmental moisture control in containers

3.2.1.1 Containers

Controlling the environmental conditions for the cement paste/mortar/concrete specimens is an important issue. Fig. 37 shows the dimensions of the containers used for the specimens.

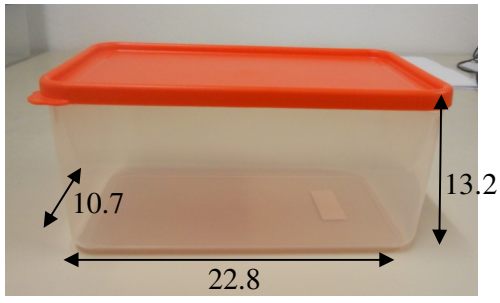


Fig. 37. Containers dimensions (cm)

3.2.1.2 Testing the salts

The environmental moisture control in the containers was achieved through the use of salt solutions, as referred before. As the volume of the used containers is different from the one in the calibrator chamber by VAISALA (mentioned in Section 3.1), different proportions of salts were tested. The salts from VAISALA´s calibrator are expensive; hence a local store of chemical products was chosen to order the same salts. Lithium chloride (LiCl), Magnesium chloride ($MgCl_2$), Sodium chloride (NaCl) and Potassium sulphate (K_2SO_4) were purchased, and common cooking salt (NaCl) was purchased as well to compare the behaviour against the Sodium chloride.

3.2.1.3 Preparing the salt solutions

The salt solutions were used to obtain different relative humidity values in each container. Two groups of 5 containers each were used (numbered 1 to 5 for the first set and 6 to 10 for the second set). In one group different salts in the same quantity were used. In the second group the same NaCl salt was used in each container, but in different quantities.

The proportions and the expected relative humidity for the VAISALA calibration system were shown in Table 1. The quantities actually used in the containers are shown in the Table 2 and Table 3. The proportion remains respect to the values showed in Table 1 for each expectable relative humidity. In the case of the containers with different salts the chosen quantity was around 50 g to get more stability on the measurements as this amount was enough to cover all the bottom of the container. On this way we avoided having the variable of the influence of the salt volume in the container in the stability of the RH readings.

Table 2. Proportions for the salt solutions used in the containers (different salts)

Containers with different salts				
Container	**Salt**	**Salt content (g)**	**Water Content (g)**	**Expected relative humidity**
1	NaCl	53.33	27.28	75%
2	LiCl	53.33	43.64	11%
3	MgCl2	53.33	5.46	33%
4	K2SO4	53.33	18.19	97%
5	Cooking Salt (NaCl)	53.33	27.283	75%

Table 3. Proportions for the NaCl solutions used in the containers

Containers with equal salt (NaCl)				
Container	**Salt**	**Salt content (g)**	**Water Content (g)**	**Expected relative humidity**
6	NaCl	20	10.23	75%
7	NaCl	30	15.35	75%
8	NaCl	40	20.46	75%
9	NaCl	50	25.58	75%
10	Cooking Salt (NaCl)	30	15.35	75%

3.3 General outline: basic principle and procedure

3.3.1 Testing RH sensors and performance of salt solutions for constant relative humidity

The salts solutions were placed in the containers 1 to 5 and were left undisturbed for 24 hours for the salts to stabilize according to the calibrating procedure recommended by VAISALA's calibrator user manual. The comparison between the sensors was also a target in this experiment, so different sensors were placed in each container (see Fig. 38). Table 4 indicates the sensors that were placed in each container.

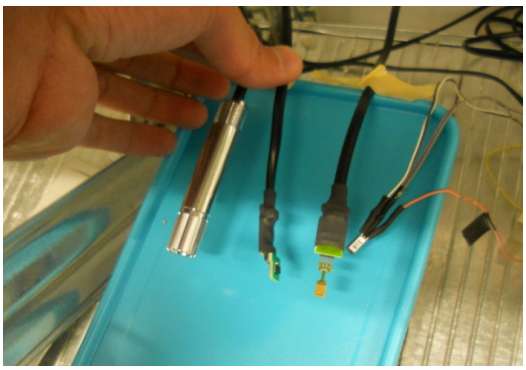


Fig. 38. Sensors ready to place inside the containers

Table 4. Sensors used for each container with different salts

Containers with different salts	
Container	**Sensors**
1	Honeywell HIH 4010 004, Vaisala, Sensirion SHT21, Sensirion SHT71
2	Sensirion SHT21, Sensirion SHT71
3	Sensirion SHT21, Sensirion SHT71
4	Sensirion SHT21, Sensirion SHT71
5	Honeywell HIH 4010 004, Vaisala

To place the sensors in the containers without affecting the internal environment, every hole or opening for passing the wiring has to be sealed. In this case tape was used to seal the gap between the cap and the container (see Fig. 39). After pouring the salt solutions, waiting 24 hours for their stabilization and installing the sensors, a period of 2 hours was necessary to allow the sensors to stabilize and start taking the measurements.

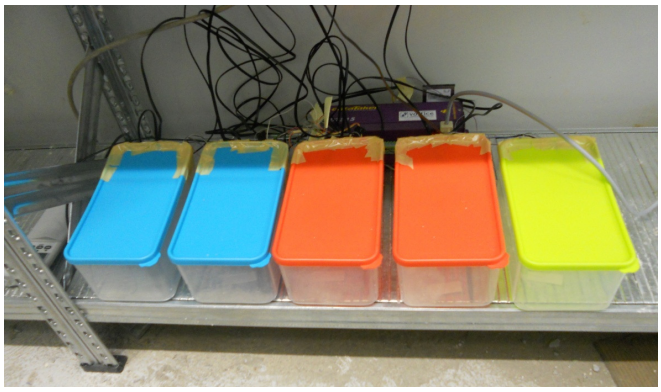


Fig. 39. Final distribution of the containers and the installed sensors

3.3.2 Test with the same salt (NaCl)

For this group of containers (6 to 10) the procedure was similar, with the difference that only Sensirion sensors were placed simultaneously in the containers 6 to 9; and only a VAISALA sensor was used in container 10 (see Table 5).

Table 5. Sensors used for each container with the NaCl salt

Containers with equal salt	
Container	**Sensors**
6	Sensirion SHT21, Sensirion SHT71
7	Sensirion SHT21, Sensirion SHT71
8	Sensirion SHT21, Sensirion SHT71
9	Sensirion SHT21, Sensirion SHT71
10	Vaisala

After 7 days of measuring a glass of water was placed in each container, to asses the eventual disruption of internal humidity in the container due to the presence of evaporating water from the glass. The glass was placed on top of a suitable base (Fig. 40), to prevent the glass from being wet by the salt solution, and allow regular weighting of the water glass for assessment of mass loss, without disturbances associated to droplets from the salt solution. The objective was therefore to check if the salt solution in the container was able to absorb the significant increase of relative humidity induced by evaporation of the water in the glass, and how it affects the effectiveness of the salt solution and its capacity to maintain the intended relative humidity in the container.



Fig. 40. Glass and base to be put inside the containers

Similar amounts of water were poured and weighed in 4 glasses (one for each container), using a high precision weight scale that was installed in the climatic chamber. Table 6 reproduces the initial glass of water weights for the experiments.

Table 6. Glass of water content for each container

Container	Glass of water content (gr)
6	44.23
7	45.99
8	44.89
9	44.82

Upon placement in the containers, the glasses of water were weighed regularly. Care was taken to minimize the disturbance to the experiment caused by opening the container and weighing the glass of water. In fact, the operation was relatively fast, and the container was kept closed while the glass was being weighed. Fig. 41 shows the glasses placed in containers 6 to 9.



Fig. 41. Glasses placed in containers 6 to 9

The relative humidity measurements continued after the water glasses were placed in the containers.

3.4 Results and discussion

3.4.1 Measurements for the containers with different salts

The readings of the sensors in each container are shown in Figures Fig. 42 to Fig. 46. The objective is to monitor the behaviour of the salts along the time, to compare the readings of

each sensor for each salt solution, and to check the influence of the containers volume on the RH measurements (based on the reference values according to the VAISALA´s relative humidity calibrator).

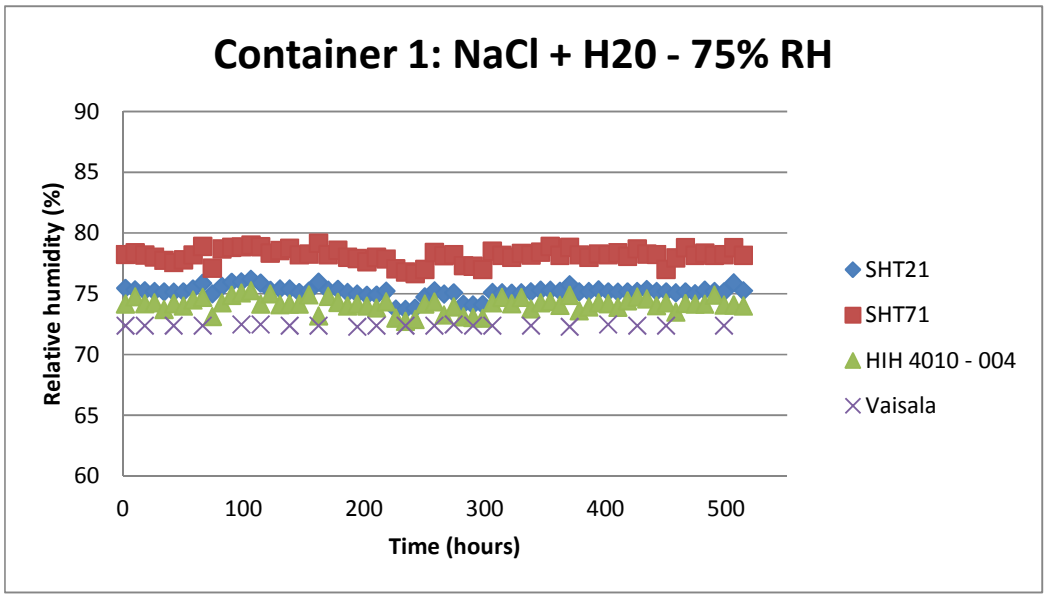


Fig. 42. Relative humidity readings in container 1 (expected relative humidity of 75%)

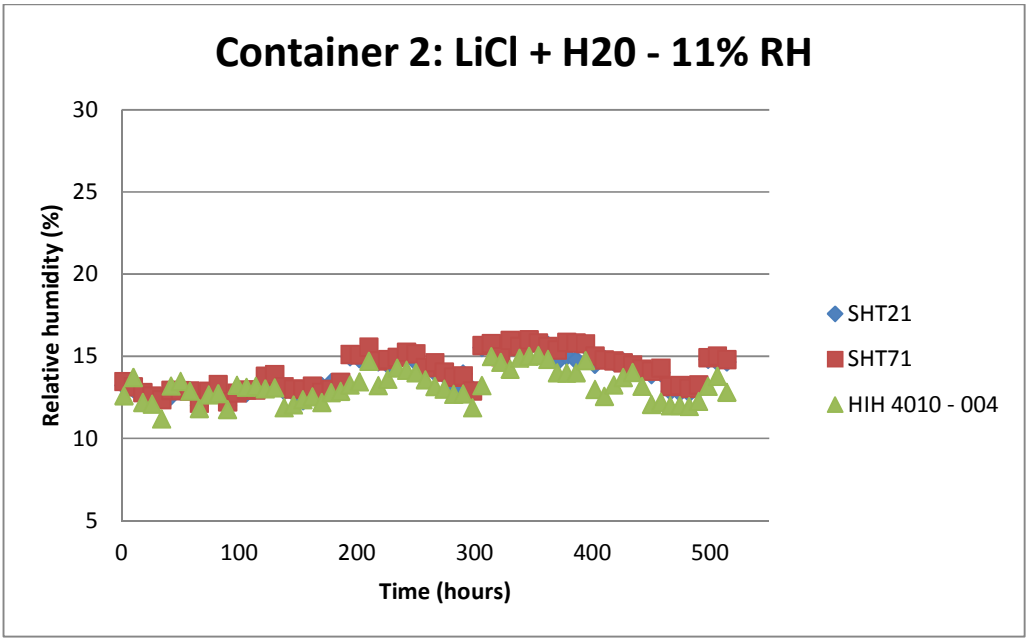


Fig. 43. Relative humidity readings in container 2 (expected relative humidity of 11%)

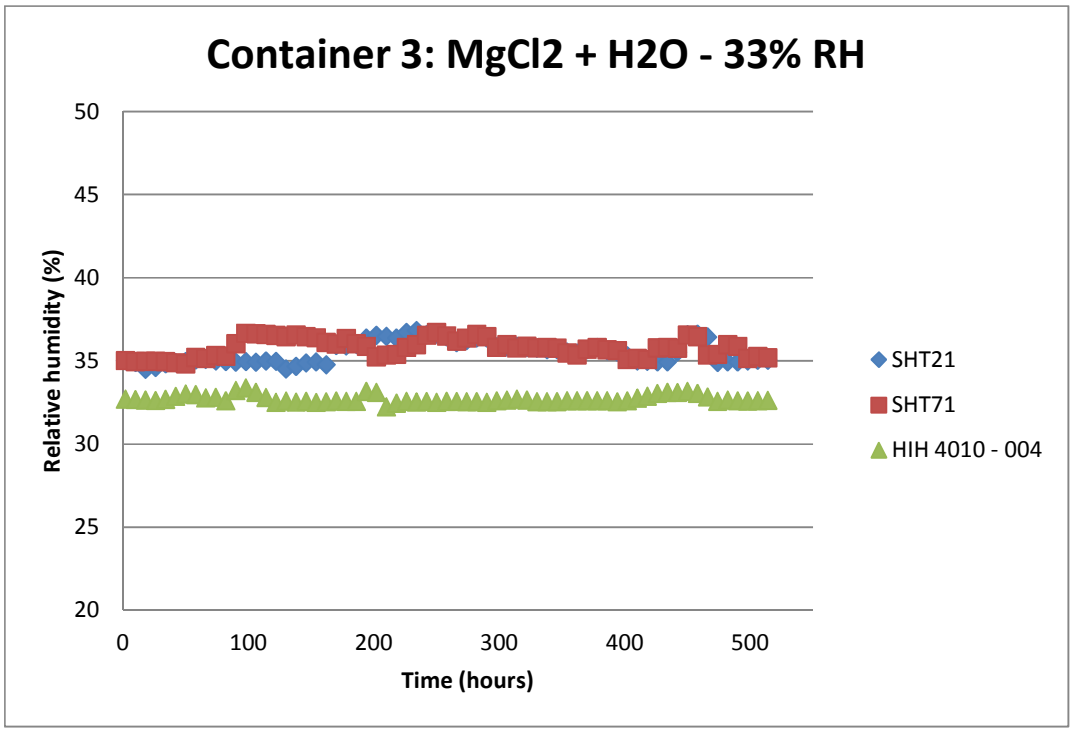


Fig. 44. Relative humidity readings in container 3 (expected relative humidity of 33%)

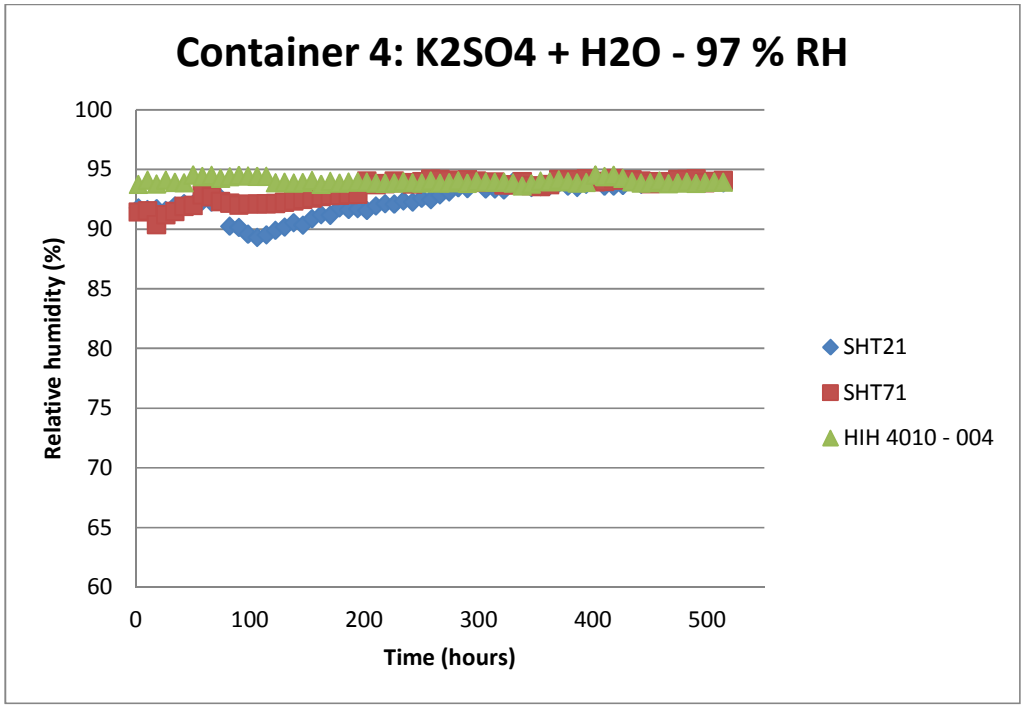


Fig. 45. Relative humidity readings in container 4 (expected relative humidity of 97%)

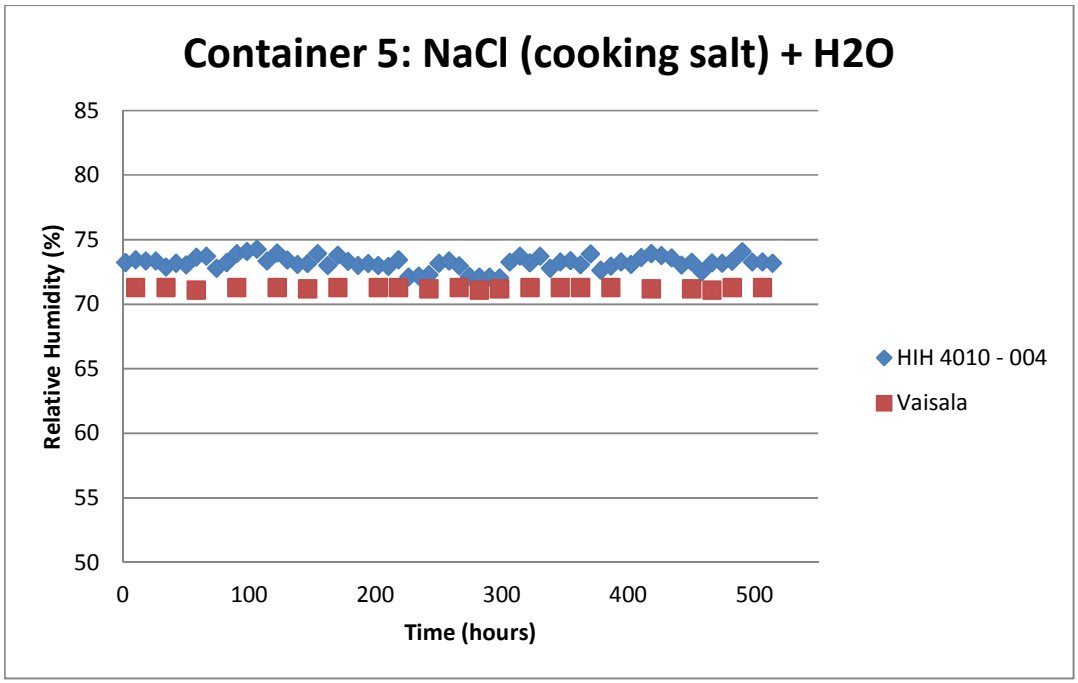


Fig. 46. Relative humidity readings in container 5 (expected relative humidity of 75%)

These figures show that it was feasible to achieve the expected relative humidity, considering that the salts could not be 100% efficient and the limited accuracy of the RH sensors. The readings show that the less stable salt solution was K_2SO_4 (targeted humidity of 97%). However the interpretation of this lower efficiency should bear in mind that the RH sensors have decreased accuracies at RH values above 90%.

Another issue, is that even if the sensors can reach those values of relative humidity (more than 90 %), they take relatively long times to attain such moisture equilibrium. That is why an initial increase of the values of RH can be seen at the beginning of the readings. This is attributable to the sensor performance and not to actual RH changes inside the container.

For the salt LiCl solution, the expected relative humidity was 11%, however, at this range of relative humidity, RH sensors could reduce accuracy or give readings slightly higher. In this case 1 to 2% higher than the expectable as is shown in Fig. 43.

Regarding the readings of the sensors, the most stable was the one from VAISALA. Its readings are useful as a reference to compare the readings of the other sensors. Usually, the behaviour of the sensors is as follows: Sensirion SHT71 gives the highest values and the lowest values are given by Honeywell sensors HIH4010. Sensirion SHT21 readings are in the middle.

Finally, in regard to the use of the cooking salt, the readings have shown that is feasible to achieve a constant relative humidity with this kind of solution. This is an important conclusion in view of establishing low-cost solutions for moisture control and testing of cement-based materials.

3.4.2 Measurements for the containers with the same salts (NaCl)

The readings of the sensor in each container are shown in figures Fig. 47 to Fig. 51. In these experiments the NaCl salt is used in the solution, and the influence of the quantity of salt in humidity control is to be assessed. The reference value is RH = 75% according to VAISALA´s relative humidity calibrator. After the glass of water is placed in containers 6 to 9 at the age of 7 days, the measurements continued from then on.

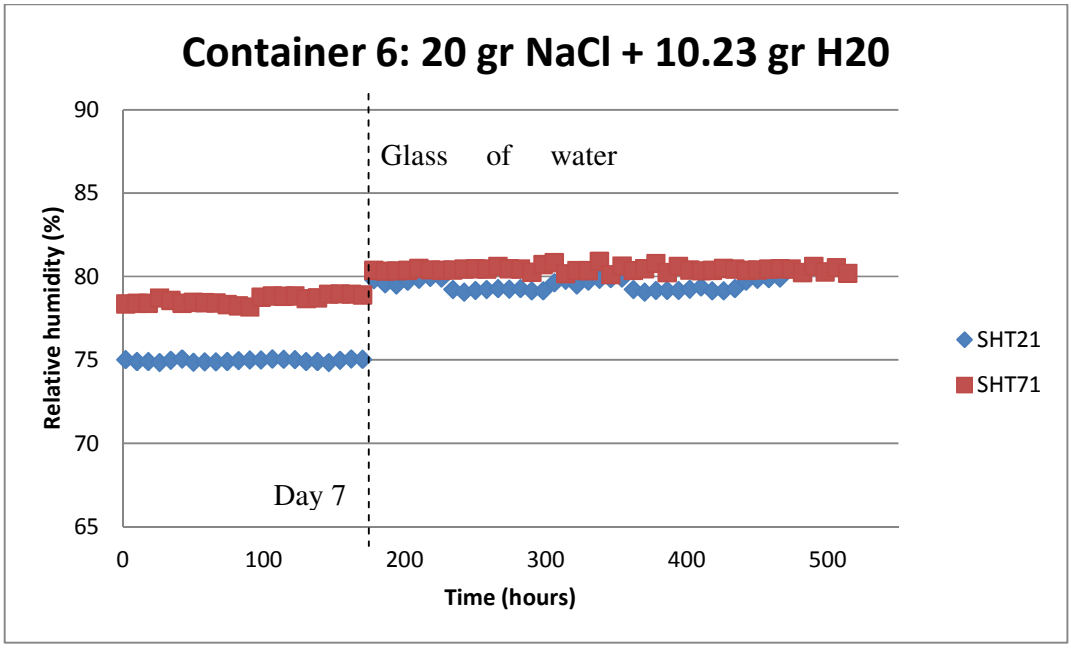


Fig. 47. Relative humidity readings in container 6 (solution for 20 gr of NaCl)

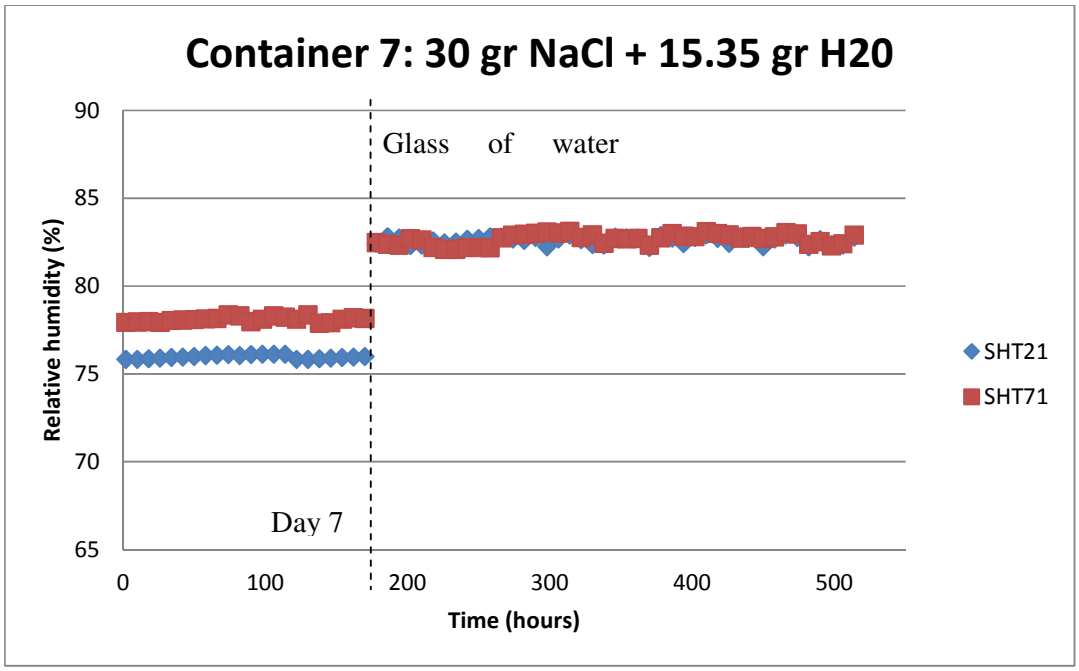


Fig. 48. Relative humidity readings in container 7 (solution for 30 gr of NaCl)

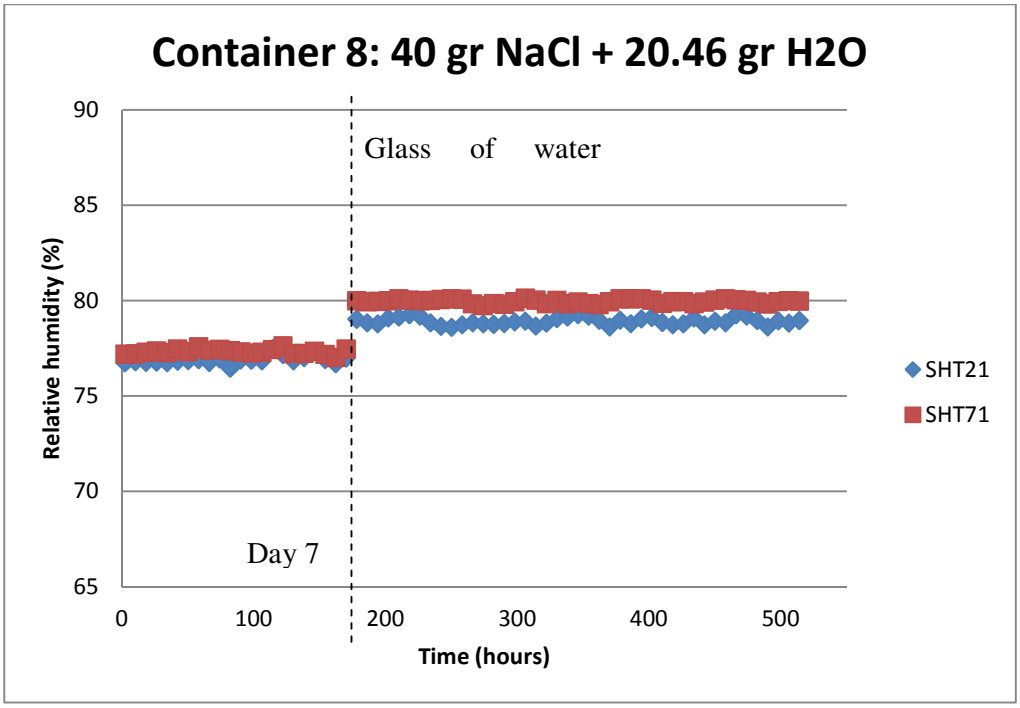


Fig. 49. Relative humidity readings in container 8 (solution for 40 gr of NaCl)

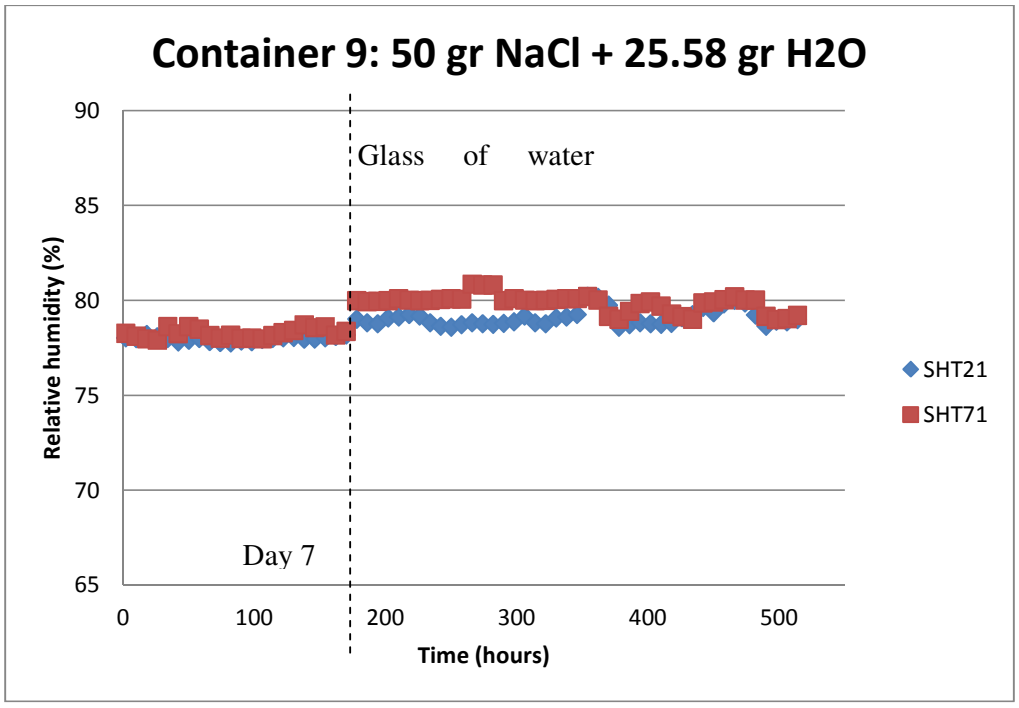


Fig. 50. Relative humidity readings in container 9 (solution for 50 gr of NaCl)

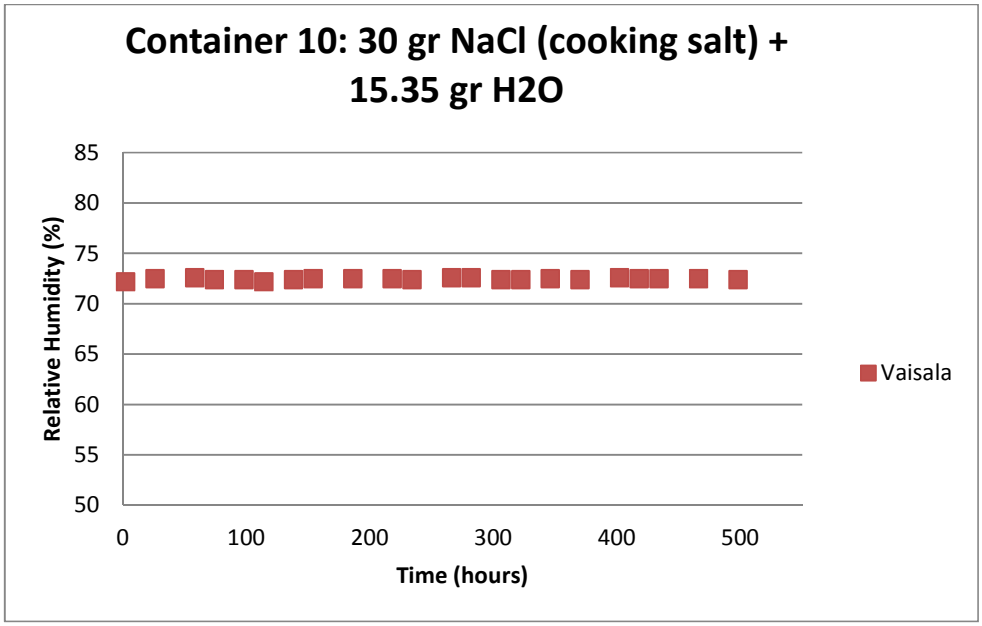


Fig. 51. Relative humidity readings in container 10 (solution for 30 gr of NaCl "cooking salt")

All the containers could provide measure values of RH near to the expected relative humidity of 75% and the quantity of salt solution did not really change the tendency to give readings near 75% RH. However, the influence of the amount of salt solutions is clear in regard to the stability of the container RH after the water glass is placed inside. The higher the amount of salt solution, the smaller the difference between the sensor readings. Hence, containers 8 and 9 (40gr and 50gr of NaCl respectively) showed more stability in the readings before placing the glass of water and a small difference between the readings of relative humidity after that.

Container 10 revealed stable readings during 500 hours (~21 days), being able to maintain the relative humidity, which confirms the feasibility of using cooking salt as an agent to create controlled relative humidity.

4 EFFECT OF GORE-TEX® PROTECTION IN MOISTURE MEASUREMENTS

This chapter regards the use of relative humidity sensors to measure moisture profiles in concrete specimens using Gore-Tex as protection to avoid liquid water to be in contact with the sensors. Preliminary works has been done in order to better understand the performance of this material aiming to use it in concrete humidity measurements. Then, longer term experiments have been conducted to represent similar conditions which the relative humidity sensors will be exposed.

The target of these experiments is to evaluate the feasibility of using Gore-Tex for protection of relative humidity sensors from liquids allowing embedment of the sensor in concrete since casting.

4.1 Testing Gore-Tex efficiency

The direct embedment of the capacitance/resistive sensor in fresh concrete would cause it to fail, due to the damage to the sensing element and electrical circuitry. Therefore, by protecting the sensor with a PVC tube, a material would be necessary to allow the passage of water vapor, but hinder the liquid water. This kind of performance requirement can be met with Gore-Tex. However, doubts exist regarding the effectiveness of sensing capacities of a sensor directly in contact with the environment in which RH is to be measured, and a sensor which is housed in a chamber, whose contact with the measuring environment is made through a Gore-Tex sheet.

Two types of Gore-Tex were used with distinct features:

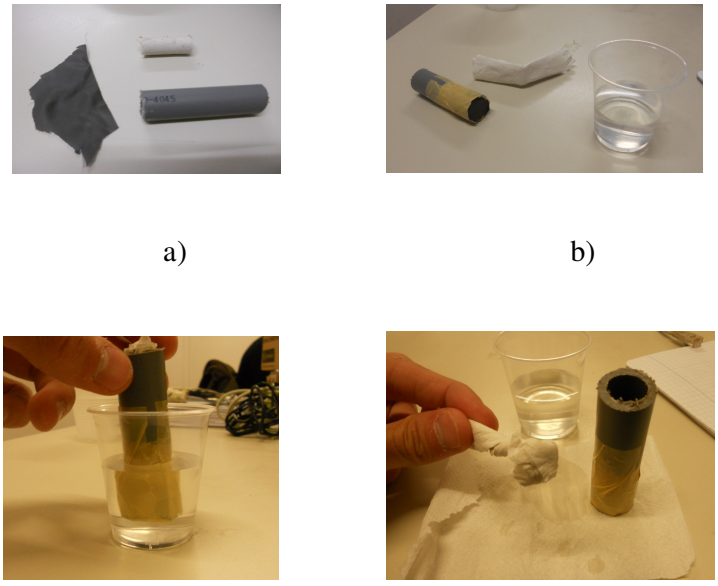
- G1: High visibility + low textile: breathability RET: <90 (x10 3) m2 mbar/watt <9 m2 Pa/W ISO11092:1993
- G2 (Military) : breathability RET: <130 (x10 3) m2 mbar/watt <13 m2 Pa/W ISO11092:1993

The Fig. 52 shows both types of Gore-Tex where G1 is the Gore-Tex with less breathability and G2 the one with more breathability.



Fig. 52. Types of Gore-Tex to be used to obtain moisture profiles in concrete

Before trying with sensors, a first experiment was done to test the reliability of Gore-Tex. A small segment of PVC tube, a piece of Gore-Tex, tape, tissue and a glass of water were necessary for this experiment. One of the edges of the tube was wrapped with Gore-Tex and sealed with tape. The tissue was inserted in the tube and then, the tube was placed in a glass of water (see Fig. 53)



a) b)

c) d)

Fig. 53. a) Gore-Tex, PVC tube and Latex cork as the sensor´s case; b) Tissue, PVC case and glass of water; c) The tube with the tissue inside blocked with the latex cork on the top and immersed in water; d) After 2 hours the tissue is removed dry

After 2 hours of keeping the tube with the tissue inside the glass of water, the tissue remained dry and the effectiveness of Gore-Tex was confirmed. In the following section the experiments using sensors are explained.

4.2 Saturation effect of the sensor after prolonged subjection to very high humidity levels

As explained above, the objective for the use of Gore-Tex is to avoid the contact within the sensor and water. However, an accurate measurement is required. According to Grasley´s work (Zachary Grasley 2006), the time response of humidity sensors protected by Gore-Tex is known to be affected, causing a delay in the RH readings or even changing the values in a small percentage.

Within the scope of this research work, it was decided to assess the delay and shift in humidity measurements caused by a Gore-Tex protection and also the response under extreme relative humidity values when using it. The sensors were placed inside a glass of water to represent the extreme relative humidity environment which would be equivalent to fresh concrete.

4.2.1 Preliminary test

A preliminary test was performed to evaluate the variables mentioned above. The RH sensors that were used for this experiment are Sensirion SHT21 (accuracy of ± 3%RH).

Initially, the 4 SHT21 sensors (named S1 to S4) were exposed to the environment without any covering to check the coherence of measurements between the sensors. Under environmental conditions in a room without any kind of climatic control for a period of 2 hours, all the sensors responded coherently, within the range 49.8% and 50.1%. This 0.3% variation is considered quite small in regard to the accuracy of the sensors and thus the response of the sensors is considered equivalent.

The experiment continued by exposing the sensors to the environment, but this time using Gore-Tex as a bounding material (Gore-Tex type G1). Sensor S1 was placed in a 1.5 cm internal diameter and 5 cm length plastic tube. One side was wrapped with Gore-Tex fixed with contact glue, the other edge was plugged with a latex cap of 2 cm allowing 3 cm to place the sensor. Sensors S2 and S3 were wrapped with Gore-Tex directly; one using tape (S2) and the other one using contact glue (S3) to fix the Gore-Tex to the sensor and wire. Sensor S4 remained uncovered for comparison.

The sensors were left for 2 hours for stabilization. The relative humidity was accurately monitored with the Gore-Tex protection, having readings within the accuracy range in comparison with the sensor without protection (S4). At this point, the sensor S1 was immersed in a glass of water. The readings shown in Fig. 54 started 30 minutes after insertion of the tube into water (time “0” corresponds to submersion”).

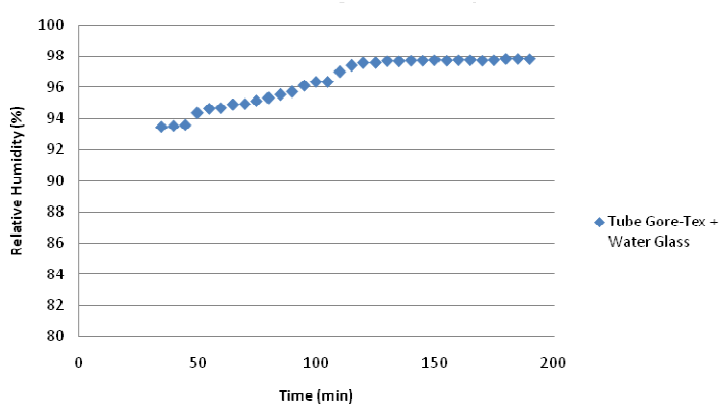


Fig. 54. Relative humidity measurements inside water

Even though a high relative humidity could be monitored by S1 (up to ~98%), which was desirable (in view of the total saturation of the air pocket inside the tube associated to submersion), the final outcome of this test was a failure due to leakage of water to the interior of the tube. In fact, after 3 hours of measurements, water could enter inside the tube, the sensor got wet and stopped working. This experiment was repeated with a replacement sensor "S5" (also SHT21), with more care being taken in regard to the sealing quality between Gore-Tex and the plastic tube (which was actually the weak point found in the first test). The use of silicone to seal the Gore-Tex and fix it in the PVC tube was really effective. This attempt was performed for a period of 9 days taking out the sensor from the glass of water at the 6th day (see Fig. 55).

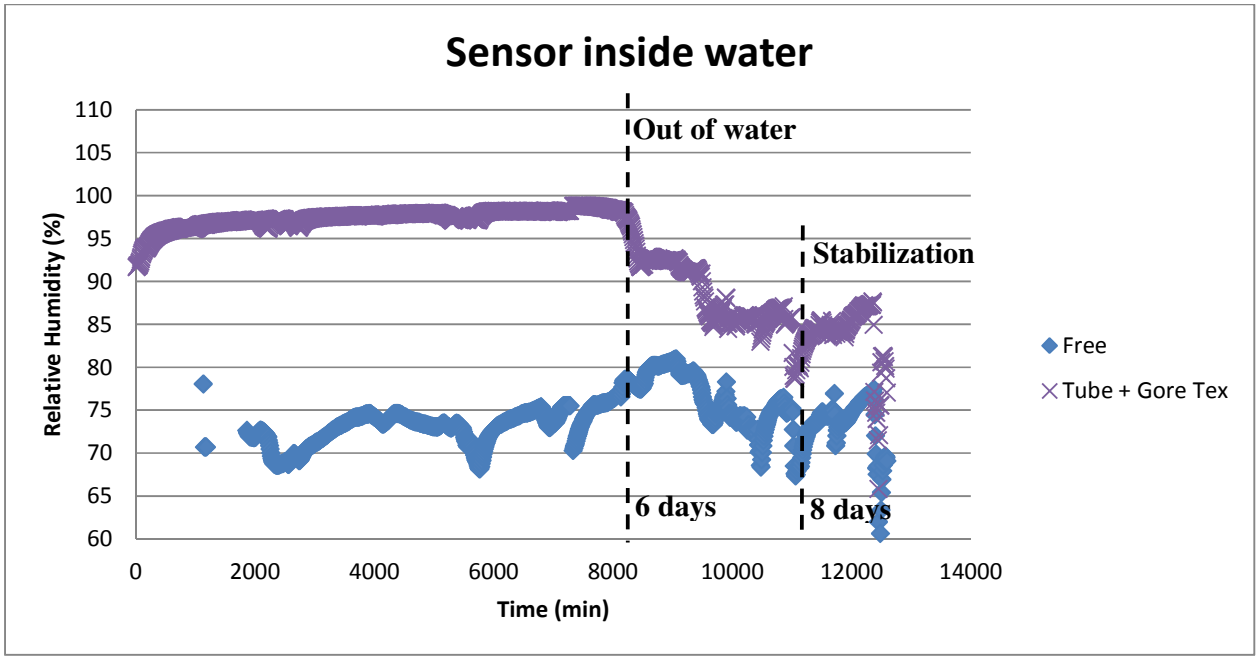


Fig. 55. RH measurements of the sensor with Gore-Tex inside water compared with a free sensor

The sensor inside the tube with Gore-Tex placed in the glass of water reached 99% RH after 5 days. The readings remained at that value for 1 day and then, the sensor was taken out from the glass of water to check the time until its stabilization with the environment. A period of two days for stabilization can be considered, when the sensor inside the tube gave a RH value very close to the measurements with the free sensor.

Simultaneously, sensors S2 and S3 continue the measurements of the environment as shown in Fig. 56. The target for these measurements is to compare the RH values given by the sensors wrapped with Gore-Tex with those ones with the free sensor. At the same time, the influence of the glue for sealing the Gore-Tex was checked.

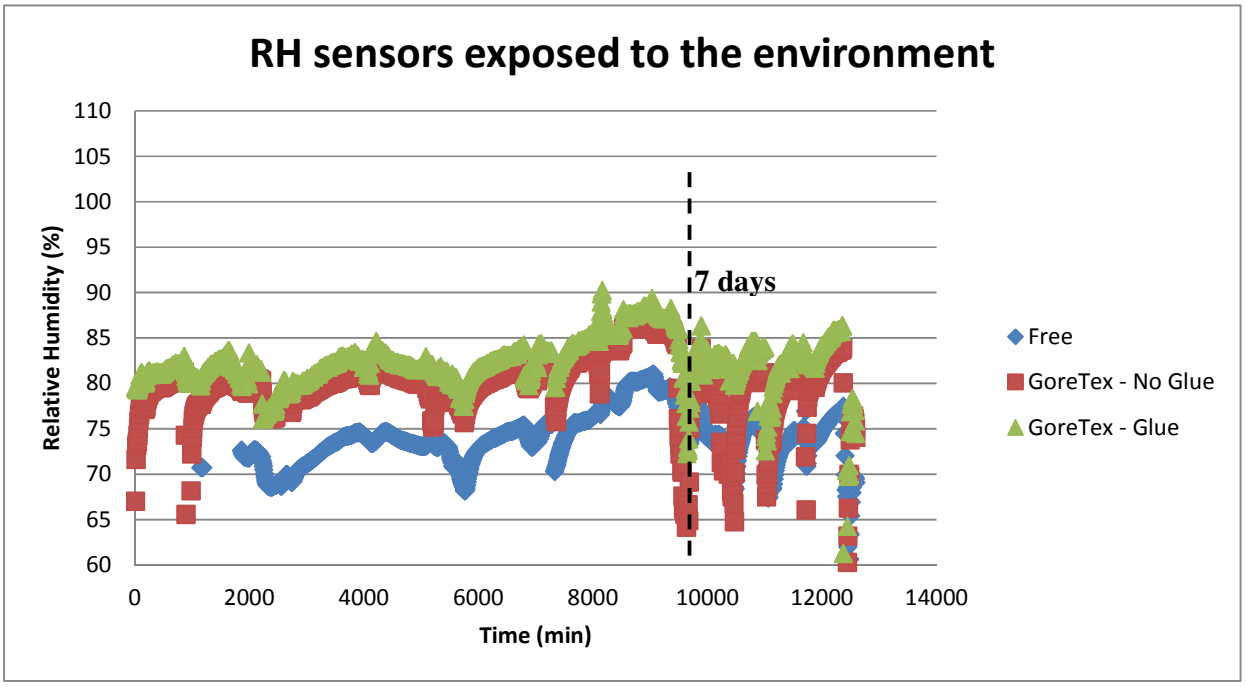


Fig. 56. RH measurements of sensors wrapped with Gore-Tex compared with a free sensor

The wrapped sensors gave similar values; hence, there is no significant influence of the glue for wrapping the Gore-Tex. Then, the wrapped sensors gave always RH values of 3% to 4% higher than the free sensor until their stabilization after almost 7 days when the difference became lesser. This could be due to condensation within the Gore-Tex and the sensor in the small space created by the Gore-Tex clothes, creating a more humid microenvironment. As this was a preliminary test, sensors S2 and S3 (wrapped directly with Gore-Tex) were not submerged in water because there was a high risk for them to get wet and stop working.

4.2.2 Second test

After the preliminary tests a better understanding of the use of Gore-Tex in RH sensors was achieved and a longer term experiment was considered necessary to get conclusions about the reliability of using Gore-Tex in moisture profile measurements.

The sensors used in these experiments were Sensirion SHT75 with an accuracy of ± 1.8%RH. They will be named S6 to S9 to continue the nomenclature sequence.

For this second test 3 variables were studied: difference within using Gore-Tex in different fashions (S6 and S7), feasibility of measuring RH inside water with sensors directly wrapped with Gore-Tex (S8) and the comparison with free sensor measurements (S9). The Gore-Tex to be used is the G1 type as in the preliminary test.

For a better understanding of the variables to be evaluated, the experiment was ment to expose the sensors to 7 stages according to the procedure shown below:

- Stage 1 (STG 1): The sensors are placed in the climatic chamber at 60% RH and 20°C without any Gore-Tex cover.
- Stage 2 (STG 2): The sensors remain in the climatic chamber but the Gore-Tex protection is installed. The sensors S6 and S7 are placed inside PVC tubes and wrapped with Gore-Tex on the same way of sensor S1 in the preliminary test. S6 uses the normal fashion and S7 the reverse fashion. Sensor S8 is directly wrapped with Gore-Tex. Sensor S9 remains free for comparison.
- Stage 3 (STG 3): Sensors are exposed to not controlled environmental conditions (outside climatic chamber)
- Stage 4 (STG 4): Sensors are placed back in the climatic chamber for stabilization
- Stage 5 (STG 5): The sensors with Gore-Tex protection are placed inside water
- Stage 6 (STG 6): The sensors are taken out from the water and placed in the not controlled environment (outside climatic chamber)
- Stage 7 (STG 7): The sensors are placed in the climatic chamber at the initial conditions to wait for stabilization

Two attempts were necessary to achieve all the stages and obtain reliable results. The following pictures show the first attempt from stage 1 to 5. Stage 6 and 7 are repetitions of stage 3 and 1:



Fig. 57. Stage 1 - The sensors are placed in the climatic room protected with tape and surrounded with bricks to avoid the wind to disturb the readings



Fig. 58. Stage 2 - Three sensors were covered with Gore-Tex and one was left free. Sensor S8 directly wrapped, S6 and S7 placed inside the PVC tube and covered with Gore-Tex in two different fashions



Fig. 59. Stage 3 - The sensors are placed in the same place, surrounded by bricks



Fig. 60. Stage 4 - The sensors were placed outside the climatic room, exposed to the environment

Then, the wrapped sensors are placed in the climatic room to stabilize.



Fig. 61. Stage 5 - The sensors covered with Gore-Tex were placed each in a glass of water. Sensor S9 was left free

In this first attempt the 7 stages could not be achieved because the sensors S6 and S8 stopped working before stabilizing at 100% RH, which means that the experiment could go just until stage 5. The following graphics show 400 hours (17 days) readings corresponding to this attempt (See Fig. 62):

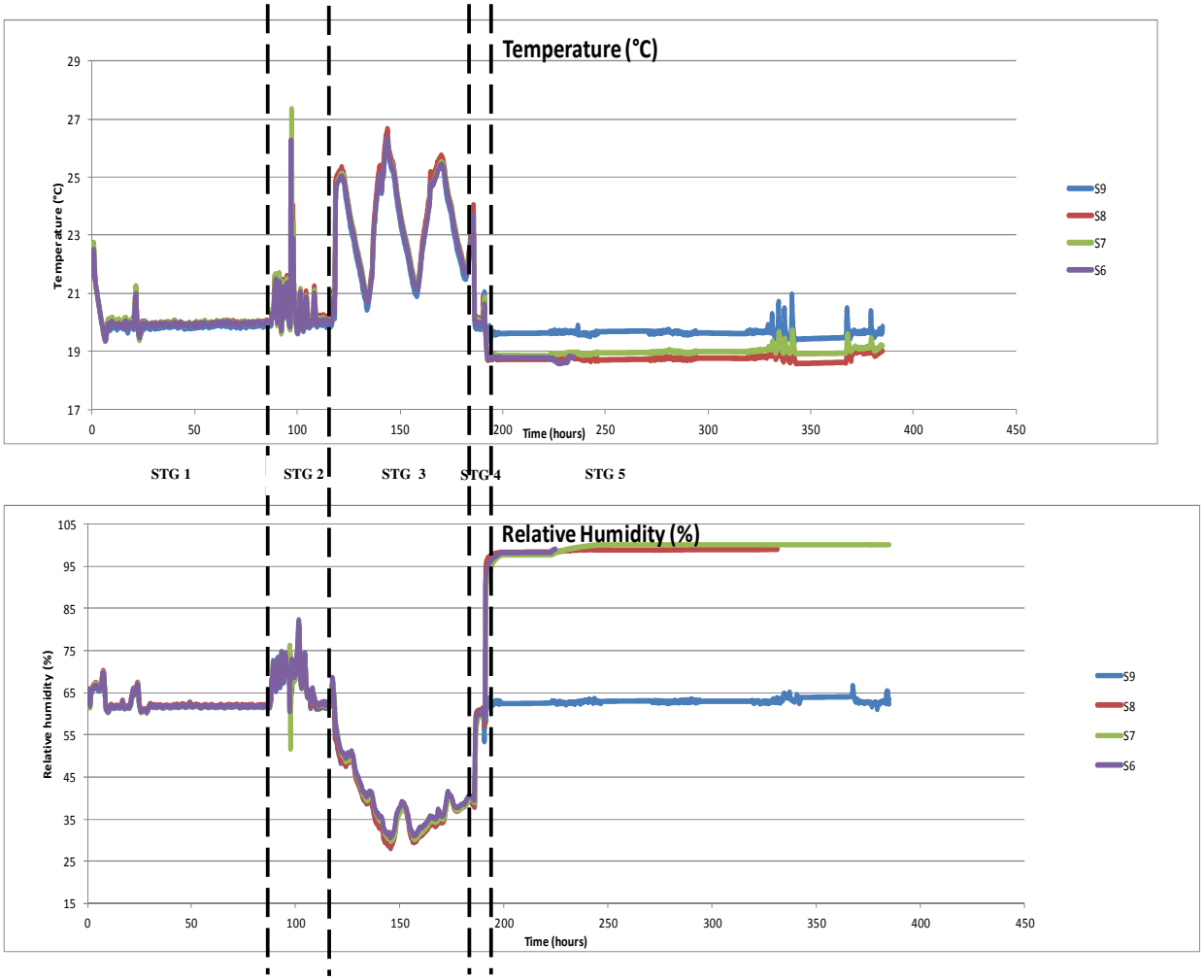


Fig. 62. Temperature and RH measurements for 17 days. Three ways of using Gore-Tex: Wrapped, Inverse fashion, Normal fashion

The response before wrapping the sensors was stable and almost the same in all sensors. Then, after wrapping, certain instability can be observed, but all the sensors continue giving similar results and uniform responses. The peaks in the readings in the stage 2 observed between t = 80 hours and t = 120 hours are due to the opening of the door in the climatic room or certain activities inside.

When the wrapped sensors are placed outside the climatic chamber in the stage 3 (t = 120 hours) the behavior within the sensors still similar and all of them respond to the environmental changes with almost no delay. These results are different from the ones

obtained in the preliminary test where the difference within measurements was higher in comparison with the free sensor measurements.

The failure of the sensors S6 and S8 was due to the sealing conditions. 3 layers of tape were used in the first attempt but it was not enough for an accurate sealing. For the second attempt the sealing was improved according to the procedure explained below. The variable of wrapping the sensor directly (S8) was not considered necessary for this attempt as the risk of losing the sensor is high and the stock was limited.

A piece of 5 cm x 5 cm piece of Gore-Tex cloth was placed on the edge of the PVC tube that was immersed in water. Contact glue was put in the edge of the tube and also in the Gore-Tex clothes. After 5 minutes the glue was dry. Then, silicone was allocated around the PVC tube near the edge where the Gore-Tex is and immediately the tube was wrapped with the sleeves of Gore-Tex. More silicone was allocated on the edges to ensure the sealing and fixation of the Gore-Tex clothes.

After the silicone is dry (around 1 minute), a second layer of Gore-Tex (3 cm x 10 cm Gore-Tex clothes) was superimposed laterally also using silicone. Finally add silicone to the upper edges to ensure sealing and fixation of the second layer. Just 1 layer of Gore-Tex should be within the bottom of the tube and the saturated environment (water or concrete in this case). The second layer must not block this part.

Fig. 63 shows the sealed PVC tube and the different fashions used in this experiment



a) b)

Fig. 63. a) Gore-Tex in inverse fashion sealed with silicone; b) Gore-Tex in normal fashion sealed with silicone

This type of sealing resulted effective and the experiment could develop all the stages thanks to that. The same type of sealing was used for the experiments with concrete specimens explained in the next chapter.

The following graphics show 58 days measurements for the three sensors as explained above. Normal Fashion, Inverse Fashion and the sensor in the Environment (see Fig. 64).

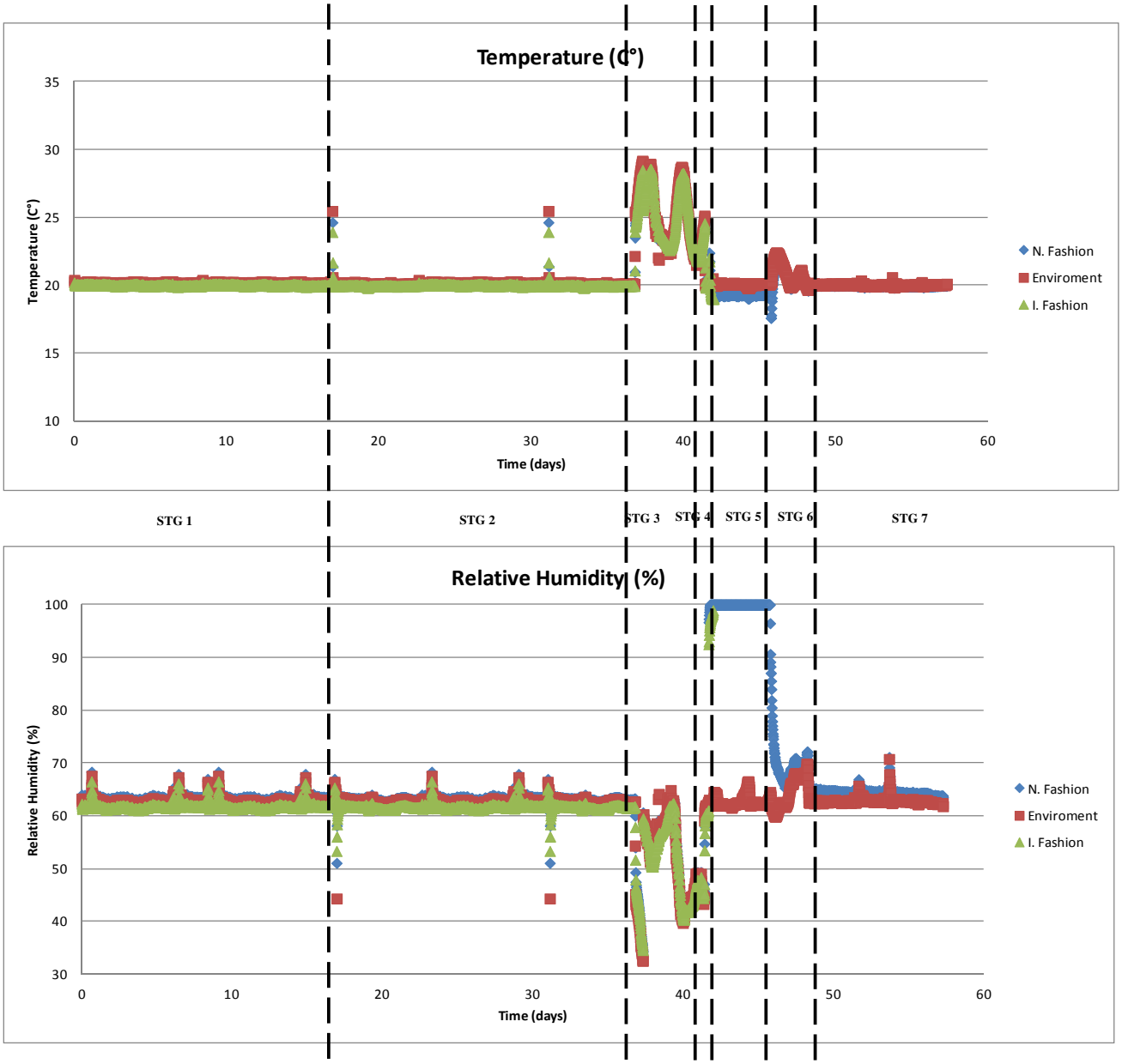


Fig. 64. 58 days temperature and RH measurements with Gore-Tex in normal fashion, inverse fashion and with one sensor leaved free

The difference within the measurements when the sensors are not immersed in water yet is in a range between 1% to 3% RH. The peaks in the measurements in the first 30 days are due to actual disturbances in the humidity inside the climatic chamber due to door opening events (people entering the chamber).

Usually, the sensor with the Gore-Tex in normal fashion gives readings slightly higher (average of 2%). This can be due to accuracy of the sensors, which would mean that there is practically no difference in using the normal fashion or the reverse one; or also because of the kind of Gore-Tex that is being used in this experiment is designed to avoid water particles to go through the material from outside to inside (normal fashion), but not in the other way around (inverse fashion). Even if the porosity is really small, the behavior towards avoiding water to pass could not the same from inside to outside. According to this concept, is possible that the enclosure of the sensor with Gore-Tex in a normal fashion makes the temperature and RH measurements to be higher. Then, practically no delay is shown in the readings of the sensors with Gore-Tex with regard to the free sensor.

For a better view of what happened when the sensors were immersed in water, a close up of the graphics is shown below (see Fig. 65).

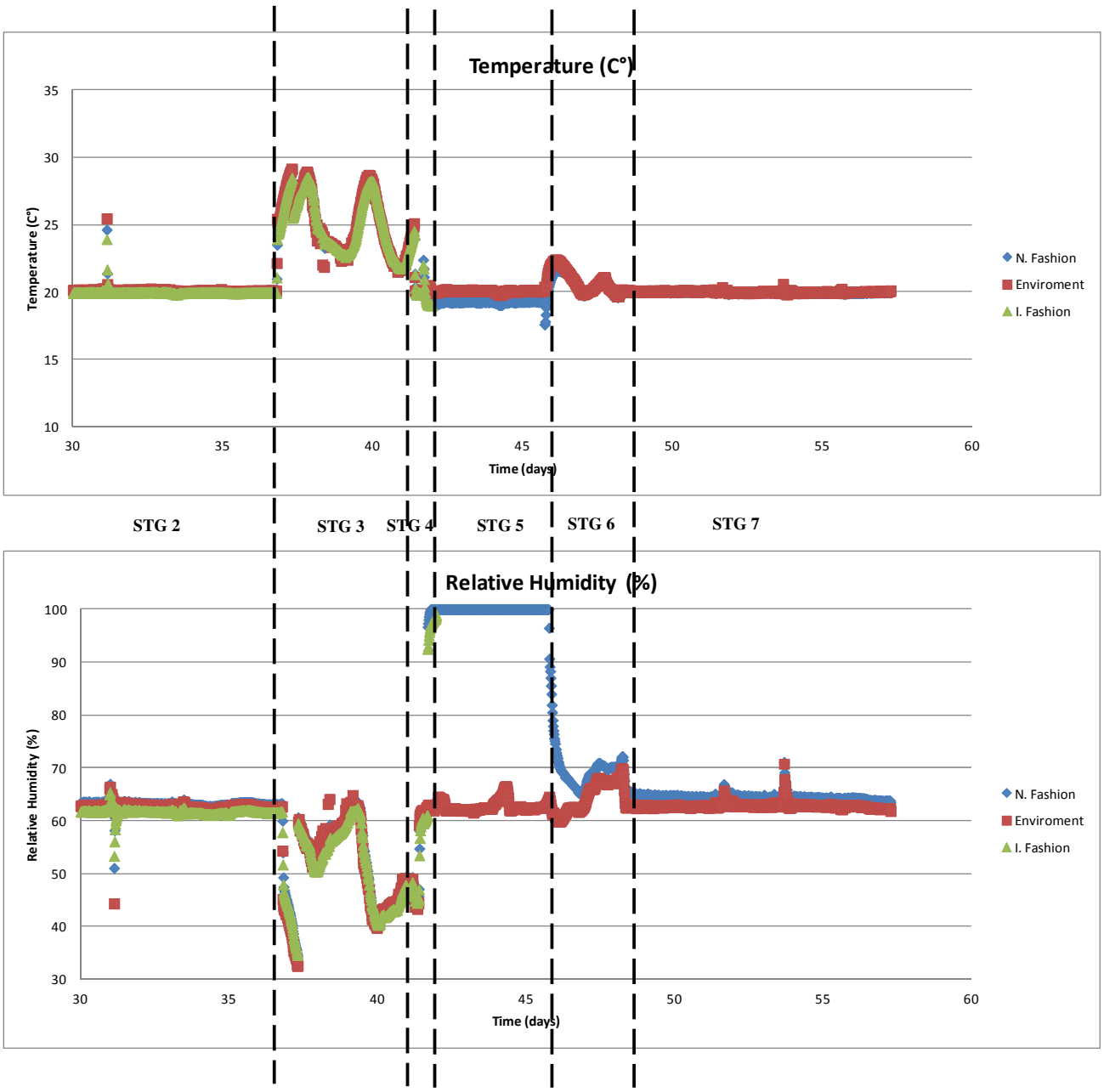


Fig. 65. Close up of previous figure for a better visibility of the sensor´s behaviour

It can be observed that the readings in all the sensors were similar during the stage 1 to 4, until the two sensors with Gore-Tex protection were placed inside water (Stage 5). In this stage the sensor with Gore-Tex in the inverse fashion (S7) stopped working. This could be due to condensation inside the tube or saturation of the sensor. The sensor with Gore-Tex protection in the normal fashion (S6) behaved better and the readings continued with the sensor inside water through all the stage 5, making possible to proceed with the next stages,

where the sensor was placed in the not controlled environment and then back in the climatic chamber. It can be observed that near the 47th day, at the middle of the stage 6 the readings of sensors S6 and S9 (free sensor) were approaching to each other, which means stabilization of the measurements for the sensor S6. This took around 18 hours after being taken out from the water.

5 LABORATORIAL EXPERIMENTS REGARDING HUMIDITY PROFILING IN CONCRETE

This chapter regards to the use of relative humidity sensors to measure moisture profiles in concrete specimens. The overall work is based on the choice of using RH sensors placed inside PVC tubes embedded into concrete. The humidity inside the tube, which is sealed except for the contact with the concrete porous network, is monitored and it should reflect the average humidity of the concrete pores.

Several experiments have been conducted in order to better understand the performance of this concrete humidity measurement approach, with particular emphasis on the test setup and test procedure.

5.1 Moisture loss measurements through relative humidity

5.1.1 Experimental set up

In order to obtain the moisture loss profile in concrete, 4 specimens were casted in the laboratory and placed in the climatic chamber at the age of 1 day. PVC tubes of 1.5 cm inner diameter and 1.8 outer diameter were embedded in the specimens at the desired depth and the

sensors were placed inside the tubes, which were in turn partially sealed with latex, creating a macro pore of known dimensions in contact with concrete.

The dimensions of the specimens are shown in Table 7:

Table 7. Specimen´s dimensions

Specimen	Length	Width	Thickness
A	60 cm	15 cm	15 cm
B	60 cm	15 cm	13 cm
C	60 cm	12 cm	13 cm
D	60 cm	15 cm	15 cm

The difference within the dimensions is due to availability of wood boards and, in the case of specimen C, because of the maximum length of VAISALA´s measuring case/probe (which is 12 cm) compared with the desired depth to be achieved. These differences in the specimen´s dimensions do not affect the comparability of specimens, as drying occurs from a single surface which is the same in all specimens.

The specimens A and B, shown below in the Fig. 66 were devised to compare 3 variables:

- Effect of the macro-pore size (also referred as ”pocket size”)
- Performance comparison of Honeywell HIH 4010 -004 and Sensirion SHT75 sensors
- Evaluation of two distinct types of Gore-Tex (G1 for hole 4 and G2 for hole 5)

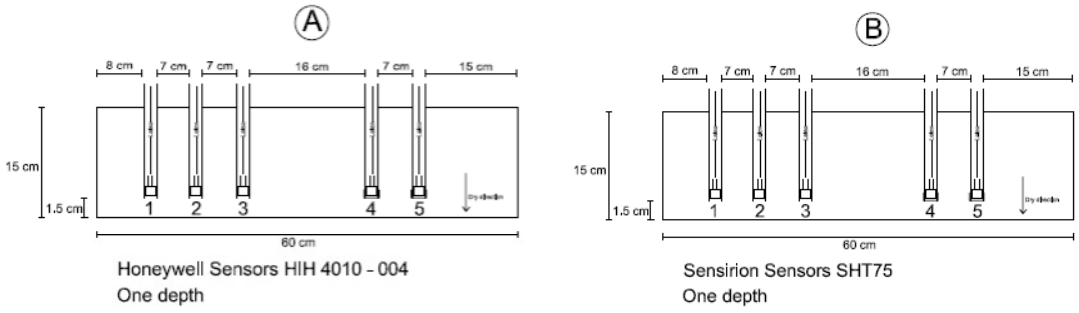


Fig. 66. Specimens A and B

In the specimens A and B, holes 1, 2 and 3 have the following pocket sizes as shown in Table 8 and Table 9:

Table 8. Pocket size for specimen A

Specimen A	
Hole 1	1.5 cm
Hole 2	2.0 cm
Hole 3	3.0 cm

Table 9. Pocket size for specimen B

Specimen B	
Hole 1	2.0 cm
Hole 2	2.5 cm
Hole 3	3.0 cm

The proportions of the pocket sizes are shown in the Fig. 67:

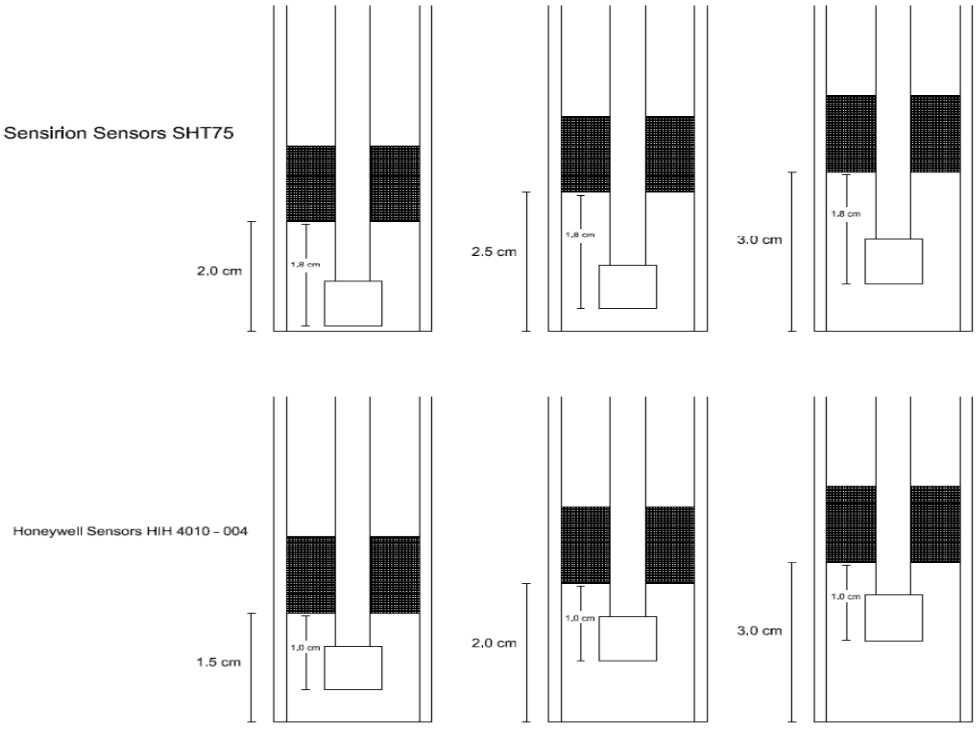


Fig. 67. Pocket size proportions for specimens A and B

The reason for having different pocket sizes in Honeywell (1.5cm; 2.0cm; 3.0cm) and Sensirion (2.0cm; 2.5cm; 3.0cm) is related to the minimum possible clearance for the sensor. Due to the fact that the Sensirion sensor is longer, the minimum pocket size that can be achieved is 2.0cm, whereas in the case of Honeywell, 1.5cm can be achieved. Therefore, it was decided to test the smallest pocket size possible in both cases. The largest pocket size was made coincident in both tests (3.0cm). The coincidence of two pocket sizes (2.0cm and 3.0cm) in both sensors will allow a relative comparison of the performance of the sensors themselves when embedded in concrete under the same conditions.

The holes 4 and 5 in specimens A and B compare the readings using different types of Gore-Tex (G1 and G2 from the previous chapter). The pocket size is 2 cm for specimens A and B, to avoid more variables.

Specimens C and D shown below in Fig. 68 compare the readings of VAISALA HM44 sensor and Honeywell sensors at 4 different depths (holes 1,2,4,5). The hole number 3 compares the readings within VAISALA sensor and Sensirion SHT21 sensor (not a Honeywell sensor due to availability issues).

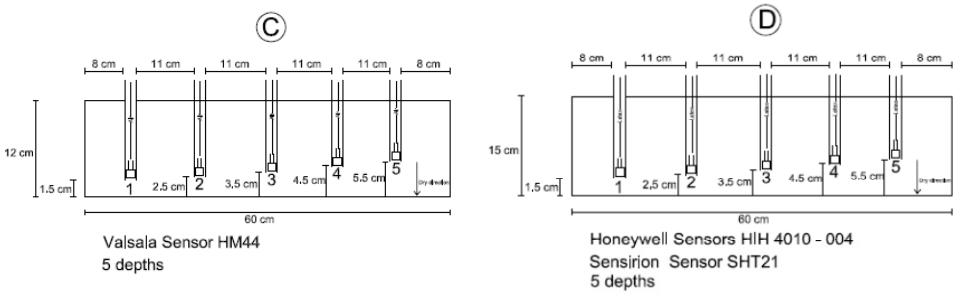


Fig. 68. Specimens C and D

The pocket size for specimen C in all the holes is according to the size of the VAISALA sensor and measuring procedure as is shown in the Fig. 69. It should be remarked that the VAISALA probe is only inserted in the sleeve for taking measurements. By default, the sleeve is kept sealed with a rubber plug.

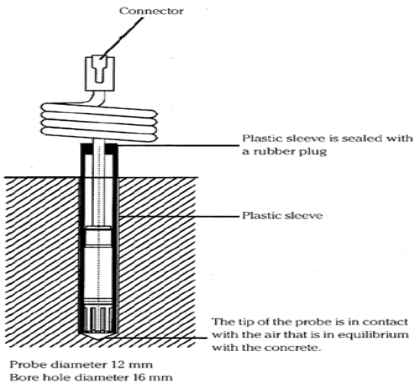


Fig. 69. Pocket size for VAISALA sensor in specimen C

The pocket size for the specimen D is 1.5 cm for all the holes. The sensor Sensirion SHT21 is smaller than the Sensirion SHT75, which is the one to be used in all other measurements with Sensirion sensors. This allows a 1.5cm pocket size for the hole 3 in the specimen D.

Table 10 shows a summary with the type of sensor, pocket size, variable to be studied and code for all the specimens:

Table 10. Sensors and variables summary for Specimens A, B, C and D

Specimen	Hole	Sensor	Variable	Pocket size	Code
A	1	HIH 4010 -004	Pocket Size	1.5 cm	HA1
	2	HIH 4010 -004	Pocket Size	2.0 cm	HA2
	3	HIH 4010 -004	Pocket Size	3.0 cm	HA3
	4	HIH 4010 -004	GoreTex G1	1.5 cm	HA4
	5	HIH 4010 -004	GoreTex G2	1.5 cm	HA5
B	1	SHT75	Pocket Size	2.0 cm	SB1
	2	SHT75	Pocket Size	2.5 cm	SB2
	3	SHT75	Pocket Size	3.0 cm	SB3
	4	SHT75	GoreTex G1	2.0 cm	SB4
	5	SHT75	GoreTex G2	2.0 cm	SB5
C	1	Vaisala	RH at diff. Depth	11.0 cm	VC1
	2	Vaisala	RH at diff. Depth	11.0 cm	VC2
	3	Vaisala	RH at diff. Depth	11.0 cm	VC3
	4	Vaisala	RH at diff. Depth	11.0 cm	VC4
	5	Vaisala	RH at diff. Depth	11.0 cm	VC5
D	1	HIH 4010 -004	RH at diff. Depth	1.5 cm	HD1
	2	HIH 4010 -004	RH at diff. Depth	1.5 cm	HD2
	3	SHT21	RH at diff. Depth	1.5 cm	SD3
	4	HIH 4010 -004	RH at diff. Depth	1.5 cm	HD4
	5	HIH 4010 -004	RH at diff. Depth	1.5 cm	HD5

5.1.2 Sealing the PVC tubes and creating a macro-pore inside the concrete specimens (Latex plug)

The sealing and macro-pore (pocket) is created using latex to block the water vapor transfer between the environment and the concrete; as well as to prevent concrete to go inside the tube. A test to ensure this and that the latex plug is airtight was conducted by placing a latex plug in the bottom of the PVC tube while leaving the top open, as shown in the Fig. 70. The age of the latex plug was 3 days. Water was poured from the top and it was checked that no water leaked from the bottom of the tube for 3 hours.



a) b)

Fig. 70. a) PVC tube filled with water and blocked with a latex cork in the bottom; b) Latex cork cup

Before working with latex, it is necessary to prepare the tubes to embed them inside concrete. For the specimens A, B and D, 5 PVC tubes were cut with a length according to the desired depth plus 5 cm. For example the tube to be placed at 1.5 cm from the surface in a 15 cm wide specimen needs to be embedded 13.5 cm inside the concrete specimen. This means that the length of the tube should be 18 cm. 13 cm for the desired depth, 1.5 cm because of the formwork thickness and 3.5 cm to ensure stability at the moment of casting.

For the specimen C (see Fig. 68), the tubes to be embedded are the VAISALA´s measuring cases, which have a constant length of 12 cm.

As preparation of the latex plug for later sealing of the actual PVC tube, the best mould is the PVC tube itself. For sealing the PVC tubes to avoid the intrusion of concrete and the water vapor transfer, a latex plug along the tube was created. For this, after cutting the tubes for each specimen, the bottom was sealed with tape. Then a 3 to 5 cm piece of PVC tube was added on the top of each tube, sealing it with tape as well as is shown in the Fig. 71.



a) b)

Fig. 71. a) 2 pieces of PVC to facilitate the latex pulling out; b) PVC pieces join together before pouring latex

For the VAISALA´s cases, tape is not necessary because the PVC piece can be added mechanically as is shown in the Fig. 72.

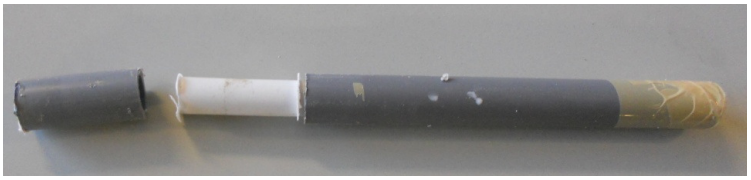


Fig. 72. VAISALA case prepared for pouring latex

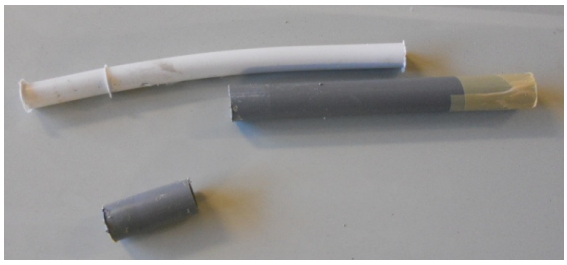
After the tubes were ready, latex was poured in the tube through the whole length, ensuring that the latex reached the top of the added piece of PVC tube. After 24 hours wait the added piece can be taken out. On this way the latex addition is used to pull the latex cork from the tube before placing the sensors. The Fig. 73 shows how the system works. The latex plug is shown outside the PVC tube just for illustration. It has to be highlighted that the plug should remain in the PVC tube until the moment of placing the sensors after the concrete specimens are hardened.



a)



b)



c)

Fig. 73. a) PVC tube with the additional piece filled with latex; b) 24 hours after the latex was poured the additional piece is removed; c) The latex plug was easily removed pulling it from the extreme

This system does not require oil or any additional device to pull the latex plug. It just use the latex properties, the Poisson effect make the latex to become thinner than the PVC tube while pulling, allowing the latex plug to come out very easy.

The next task is to create the macro-pore or “pocket” inside the tubes in the specimens A, B and D as was shown in Fig. 67 , a 2 cm latex plug together with the sensor was used. To do this, 3 to 5 cm piece of PVC tube of the same diameter was cut to be embedded in the specimens (1.5 cm diameter). The sensor wire was placed in the tube with the sensor coming

out around 3mm from the edge of the tube on the other edge. The sensor is protected with tape or any cover. Then, the bottom is sealed with tape fixing the wire as shown in the Fig. 74.

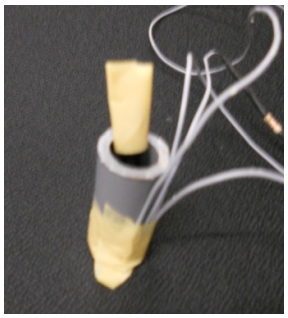


Fig. 74. Piece of PVC tube prepared for creating the latex cork in the sensor

After this, the latex was poured from the top trying to do not touch the sensor, even if it is protected. 24 hours later the plug can be taken pushing it from the PVC tube with a stick that will not damage the latex plug (round or flat point).

After having the sensor and the latex plug, the part of the latex opposite to the sensor was cut with careful of not touching the wires (cutting just by the sides and then pulling the latex remaining), making a 2 cm plug. This length ensures that the sensor is able to be inserted in the PVC tube by pushing it until the desired depth and that it is tight enough to avoid water vapor and liquid transfer within the concrete and the environment and the other way around. To place the sensor at the required depth, the distance of the tube was measured and then minus the pocket size in the sensor (sensor plus wire) and marked it. Then, the plug was pushed until the mark in the sensor´s wire is at the same level of the edge of the tube as shown in the Fig. 75.

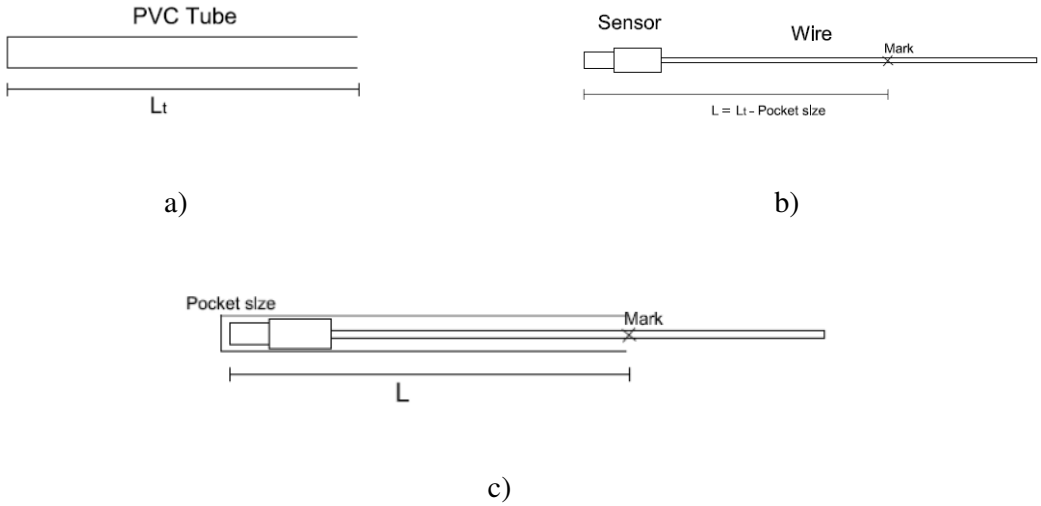


Fig. 75. Procedure for placing the sensor with the plug at the desired depth: a) Measure the PVC tube; b) Measure the desired depth in the sensor´s wire according to the pocket size and mark it; c) Insert the sensor in the PVB tube until the mark in the wire is in the edge of the PVC tube

After these tests, the PVC tubes were ready to be installed in the concrete specimens, as will be explained in the following chapters. After the PVC tubes are placed in the formwork, the additional 3 to 5 cm tube pieces are placed on top using tape as fixation (as in the procedure for sealing the tubes before casting). Then, the latex is poured until the top of the tube plus the additional piece. This ensures isolation in regard to the surrounding environment. Fig. 76 shows how the latex plug with the sensor looks like inside the tube. The concrete cast can proceed after this.

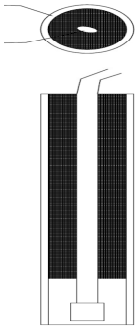


Fig. 76. Sensor and latex plug placed in the PVC tube

In the specimens A and B, the holes number 4 and 5 were wrapped on the bottom with two different types of Gore-Tex as the procedures in the previous chapter.

5.1.3 Sensor tests

After the sensors with the latex corks were ready, they were placed in the climatic chamber for half a day to check if they were working correctly.

The sensors to be used in specimen B and the hole SD3 (see nomenclature in Table 10) in the specimen D (Sensirion) were tested using the Sensirion data logger. 6 Sensirion sensors had to be tested and the Sensirion data logger has just 4 interfaces, so 4 of them were tested one half of the day and the other 2 in the other half.

For the specimens A and D, 9 Honeywell sensors were tested using a general purpose data logger: a Datataker DT80. This datalogger allows 20 connections so all the sensors could be tested simultaneously.

5.1.4 Preparing the formwork

The inner dimensions of the formworks are 15cm x 15 cm x 60 cm (see Fig. 77). These dimensions were chosen due to the availability of these formworks in the laboratory, as they had already been prepared and used for previous experiments.

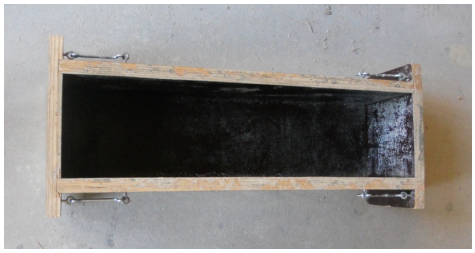


Fig. 77. Formwork for the specimens

The Fig. 78 helps as a guide to explain the casting and sealing procedures, by establishing a nomenclature to the specimen´s surfaces.

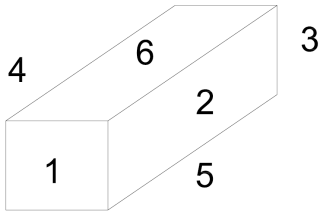


Fig. 78. Guide of the Specimens faces by number

For the specimens A, B and D, 5 holes were drilled in the wood board of the side 2. The distance within the holes has been shown in section 5.1.1. The holes have 1.8 cm diameter to create a tight space to place the PVC tubes.

The surface of the tube was made rough by making small cuts with a knife, to create adherence within the concrete and the PVC tubes. Then the tubes were placed in the holes until the depths shown in section 5.1.1. After the tubes were placed in the formwork, the borders and the little spaces within the wood and the hole were sealed with silicone.

The Fig. 79 shows 3 tubes placed in the wood formwork fixed properly and prepared for cast.



Fig. 79. PVC tubes with Gore-Tex placed in the formwork

5.1.5 Handling the specimens after casting

The concrete mix that was used in the present research follows the proportions showed in Table 11. The mix was chosen as it represents a common concrete mix used in Portugal. Table 12 and Table 13 show the concrete volume calculations and the aggregates corrections.

Table 11. Concrete mix

	Concrete mix (kg/m^3)
fine sand	245
medium sand	786
Coarse 6/14	417
Coarse 14/20	478.5
Ciment SECIL I 42.5R	280
Water	143
w/c	0.5

Table 12. Concrete volume for specimens A, B, C and D

Relative Humidity					
	Dimensions				
Specimen	Lenght (m)	Height (m)	wide (m)	Volume/unit (m3)	Volume (m3)
A	0.6	0.15	0.15	0.0135	0.0135
B	0.6	0.15	0.13	0.0117	0.0117
C	0.6	0.13	0.13	0.01014	0.01014
D	0.6	0.15	0.15	0.0135	0.0135
	Concrete Volume (m3)		0.04884		

Table 13. Aggregates correction

			Correction	
	(Kg/m3)	Quantity (kg)	X 1.2	X 1.15
fine sand	245	11.97	14.36	13.76
medium sand	786	38.39	46.07	44.15
Coarse 6/14	417	20.37	24.44	23.42
Coarse 14/20	478.5	23.37	28.04	26.88
Ciment SECIL I 42.5R	280	13.68	16.41	15.73
Water	143	6.98	8.38	8.03
w/c	0.5	0.02	0.03	0.03

The casting was made under uncontrolled conditions in the laboratory. Immediately after casting the specimens were sealed with a plastic sheet added to the concrete surface and then another plastic layer was placed to ensure that there is no moisture transfer with the

environment as is shown in the Fig. 80. The sealed specimens were placed in the climatic chamber 24 hours later at 60% RH and 25°C.



Fig. 80. Concrete specimen covered with plastic to avoid moisture transfer

After 7 days of casting, the plastic sheets and the formwork were removed (specimens A, B, C, D), except for the side 2, where the tubes were installed. Faces 1, 6, 3 and 5 were covered with paraffin wax leaving just face 4 as a drying surface.

5.1.6 Relative humidity monitoring

At the age of 7 days, the latex plugs were taken from specimens A, B and D and the RH sensors were placed according to the procedure showed in the previous section.

The monitoring for the specimens A, B and D was programmed to be every 20 minutes, because of the use of Honeywell sensors and the corresponding autonomous datalogger (Datataker DT 80G) and the Sensirion sensors datalogger. However, for the specimen B, the data collection was made separately with 1 day difference: 1 day for the holes 1, 2 and 3 and for the following day the holes 4 and 5. In the case of the specimen C, the use of VAISALA sensor just allowed measurements at discrete instants of time. Each measure required 2 hours for stabilization of the sensor, so 5 measurements per day were taken: 1 hole every 2 hours until completes the 5 holes. The latex corks were taken out from each hole in the specimen C at the moment of the measurement. Once the latex plug was taken out for the first time, the rubber plug was placed on top of the VAISALA´s cases as is shown in the section 5.1.1.

This frequency of measurements (at least one measurement per day) was necessary for 1 week to check the initial moisture loss in the concrete specimens. After 1 week, the measurements were two times a week for a period of 3 weeks. After 1 month of monitoring the relative humidity in the specimens, the measurements were once a week. The decisions on measurement frequency changes were always made according to the observed RH gradients.

5.2 Moisture loss measurements through the gravimetric method ("Slice test")

5.2.1 Expermental set up

7 concrete cylinders of 11 cm diameter by 15 cm length were casted to determine the moisture loss at different depths in concrete through a gravimetric method, with reference to the procedures mentioned in the state of the art (chapter 2). This is a destructive technique where the concrete specimen has to be destroyed at different ages that in this case were 7, 14 and 28 days. The testing should include longer time to obtain a better internal moisture distribution, but due to time limitations in the present research this was not possible.

The quantity of water was determined by weighing 3 cm concrete slices that belong to the depths of the specimens after drying in the oven until a constant weight was obtained. This gave the moisture loss profile along the time of the concrete specimens.

5.2.2 Create the "Concrete Slices"

11cm inner and 11.2cm outer diameter PVC tube were sawed to be used as a formwork to create the 11cm diameter concrete cylinders. One of the edges was taped and the other left free for casting the concrete.

Immediately after casting, the surface of the specimens was sealed with two layers of plastic on the same way of the specimens in section 5.1. After 1 day, the cylinders were placed in the climatic chamber for 7 days when the plastic sheets were also removed. The formwork and

the sealing at the bottom remained until the age of testing for each specimen which is at the day 7, 14 and 28 as mentioned above.

To test the cylinders, first the plastic sheets were removed and then the formwork was taken out cutting it with care of not cutting the concrete cylinder. After the removal of the formwork, 2 cm depth lines on the sides of the specimen every 3 cm were sawed. The sawing was made in dry condition (without adding water to the system) to do not affect the moisture conditions of the specimen. However, elevated temperatures in the saw could consume water from the concrete. This is the main reason for just slitting the specimen, instead of cutting it entirely. Following to this principle, after the 2 cm saw, a strong impact with a hammer and a chisel was made to separate the 3 cm thick slice from the specimen. Each cylinder was divided in 5 slices. The Fig. 81 illustrates the idea:

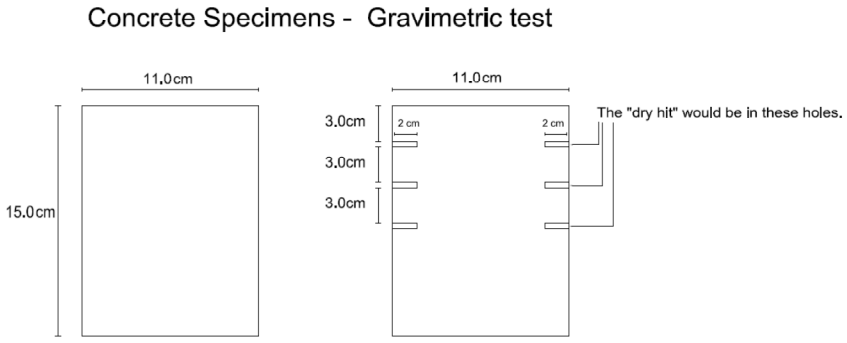


Fig. 81. Illustration for the gravimetric test

The 5 concrete slices from the specimen were placed in the oven at 105 °C to obtain the water content for each slice, which means, water content at each depth. The Fig. 82 shows the size of the slice.



a)



b)

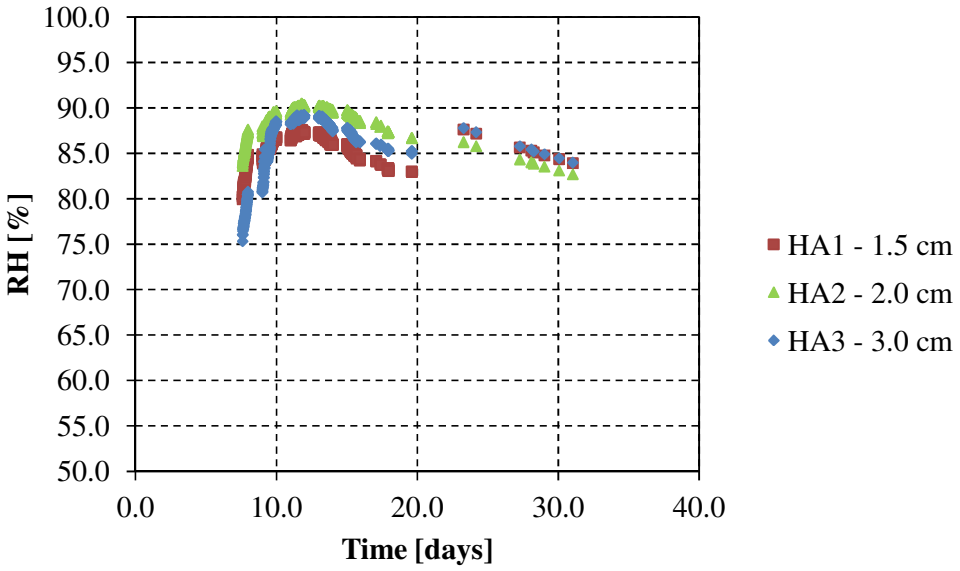
Fig. 82. a) Concrete slice after dry hit; b) The sawing should be 2 cm

5.3 Results for relative humidity profiles

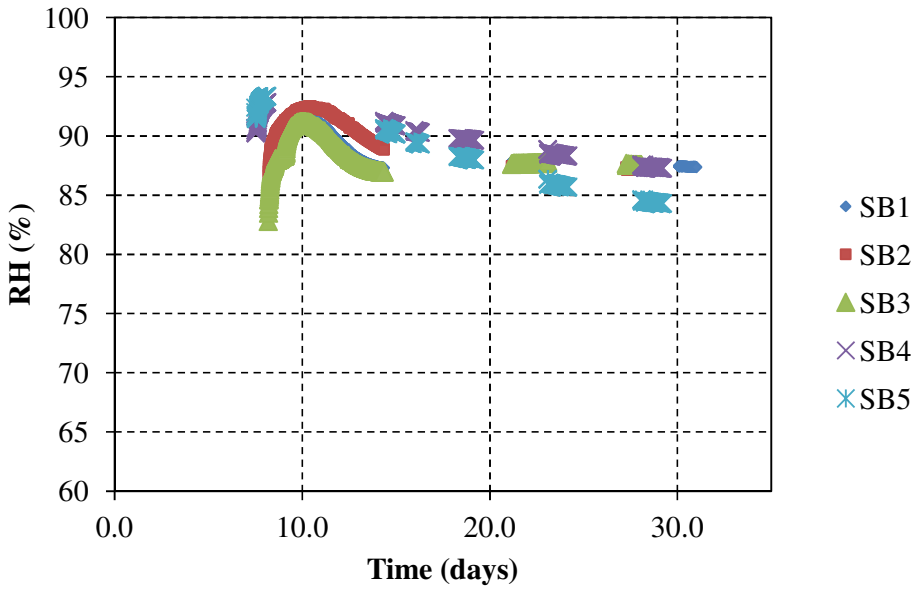
5.3.1 Specimens A and B

The following graphics compare the readings of Honeywell and Sensirion sensors in two concrete specimens (Specimen A and B), with dimensions of 15x15x60 cm each, for 2 different variables: different pocket size (See Fig. 83) and different type of Gore-Tex (Fig. 84).

First, the results for different pocket size measurements are shown for specimen A (Honeywell sensors) and specimen B (Sensirion sensors). The testing was only for 30 days because it was interrupted due to the strange outcome, in order for a re-start in a different research.



a)



b)

Fig. 83. a) RH readings of different pocket size in specimen A - Honeywell sensors; b) RH readings of different pocket size in specimen B - Sensirion sensors

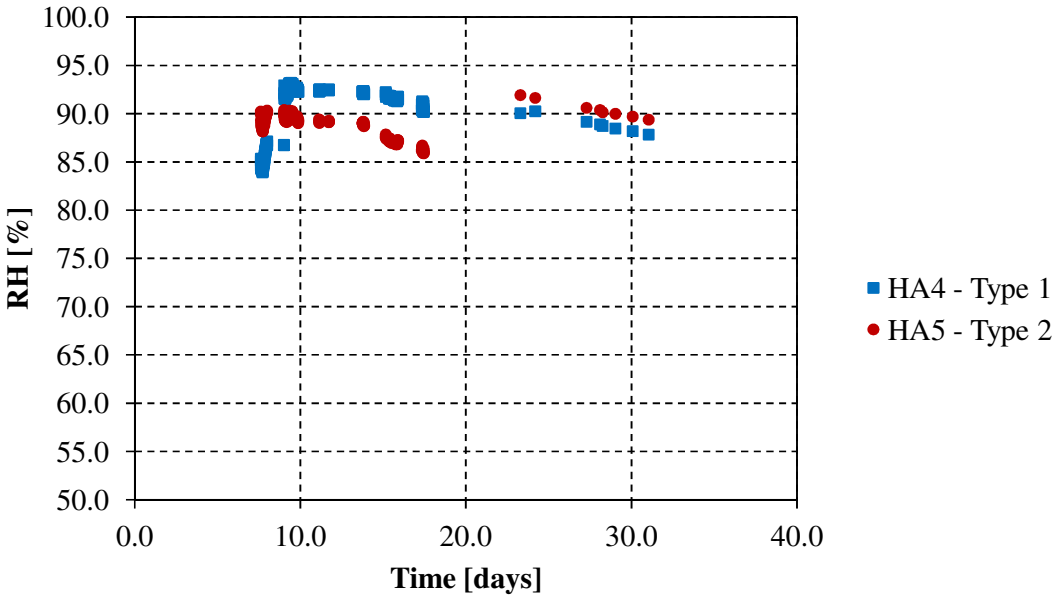
Despite of the strange outcome, the measurements were feasible. The expected outcome was to get high relative humidity at the initial stage and continuous drying process. The results show around 5 days to climb to RH values above 90% and a discontinuous drying process during the following 30 days. Considering the accuracy of the sensors (± 3%) and the short time of the experiments, it is difficult to the get final conclusions about the influence of the pocket size in the moisture profile. For example, for the sensors SB1, SB2 and SB3, the tendency should be to dry faster than SB1, SB4 and SB5. In the first 30 days this had not been shown.

The same behaviour has been found in all the specimens. However during the calibration of the sensors, the behaviour was accurate. All the readings were within the sensors accuracy when they were tested in the climatic chamber (constant RH and Temperature). The errors could be due to lack of sealing, malfunctioning of the dattaloggers or problems with the sensors when they are inside concrete.

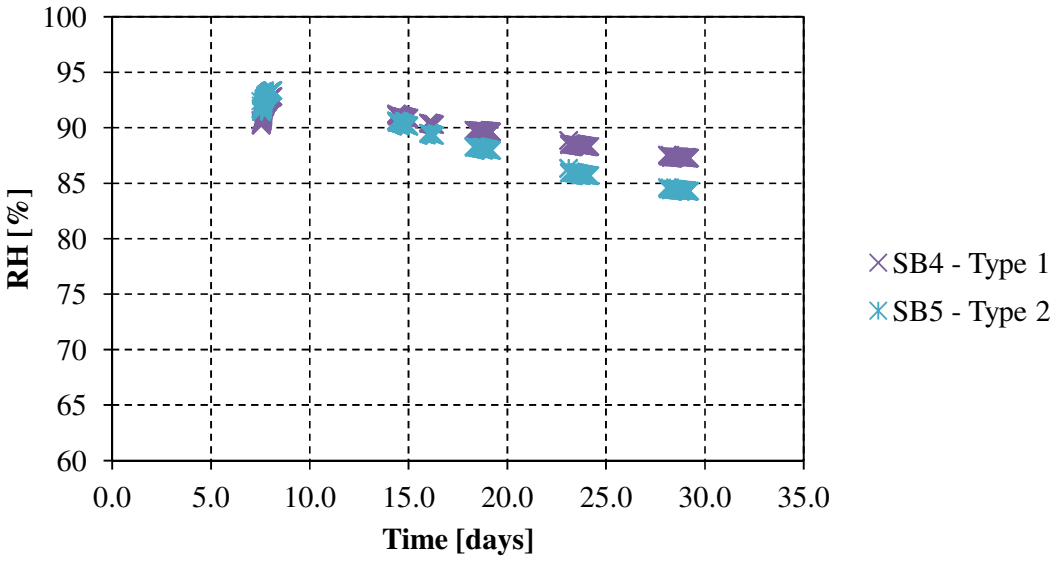
In general, there is a tendency for the Honeywell sensors to give lower readings than Sensirion sensors. The difference gets smaller with the time, but the tendency remains. The differences are up to 6 %RH at the beginning of the measurements and decrease until 3 %RH after the second day.

In Specimen A, the smaller pocket size (1.5 cm) gave higher readings than the bigger one (3 cm) until the first day, but after that, the readings were always smaller. The intermediate pocket size (2cm) gave always higher readings than the other two pocket sizes. The same happened in the specimen B, a small difference within the readings for the smaller and the bigger pocket sizes, even smaller than in specimen A. This could be due to the accuracy of the Honeywell HIH 4010 010 sensors in specimen A, which is ±3.5% RH, while in the specimen B, the accuracy of the Sensirion SHT75 is ±1.8 %RH.

The other variable for comparison in these 2 specimens is the presence of the 2 types of Gore-Tex. The Fig. 84 shows such comparison for Honeywell and Sensirion sensors:



a)



b)

Fig. 84. a) RH readings of different type of Gore-Tex in specimen A - Honeywell sensors; b) RH readings of different type of Gore-Tex in specimen B - Sensirion sensors

The graphics show similar behaviour in specimens A and B in the first 18 days of measurements. The picks are 92% and 90% for HA4 and HA5 and; 92% to 93% for SB4 and SB5. These results are within the sensors accuracy (±3%) so it can be considered that there is no significant difference when using different types of Gore-Tex. Despite of the discontinuity showed after day 24 in the specimen A, the difference in the readings still within the sensors accuracy. Regarding the discontinuity, it was not expected and could be due to the data logger used for Honeywell sensors, Data Taker, which seems to be less stable than the one for Sensirion sensors used for the specimen B, where no discontinuity was shown and the readings remained within the sensor´s accuracy. During many preliminary tests in this research work, some inconvenients were presented with the connections, the memory storage, calibration with the current or problems with the transformer. Despite of this issue, the results are presented as the scope of this research is also to show potential problems when measuring moisture inside concrete. Considering the accuracy of the sensor, the use of different type of Gore-Tex is negligible.

5.3.2 Specimen C

The results are not shown for this specimen as there was a technical problem with the VAISALA sensor. The wire that connects the sensor with the data logger was affected due to repetitive manipulation of the sensor. The sensor had to be placed in 5 different holes every hour. To take out the sensor from the VAISALA case/probe the rubber plug had to be taken out followed by taking out the sensor holding it from the wire (the is no other way of take out the sensor because it fits exactly in the VAISALA case). This procedure was repeated in previous experiments causing fatigue in the wire, ruining the calibration of the sensor.

After the sensor failure, it was considered to continue the measurement with VAISALA sensors, but the results were too different from the ones with VAISALA sensor.

5.3.3 Specimen D

Fig. 85. RH readings at different depths for specimen DFig. 85 shows the readings at 5 different depths with Honeywell sensors and Sensirion sensor in the case of HD3:

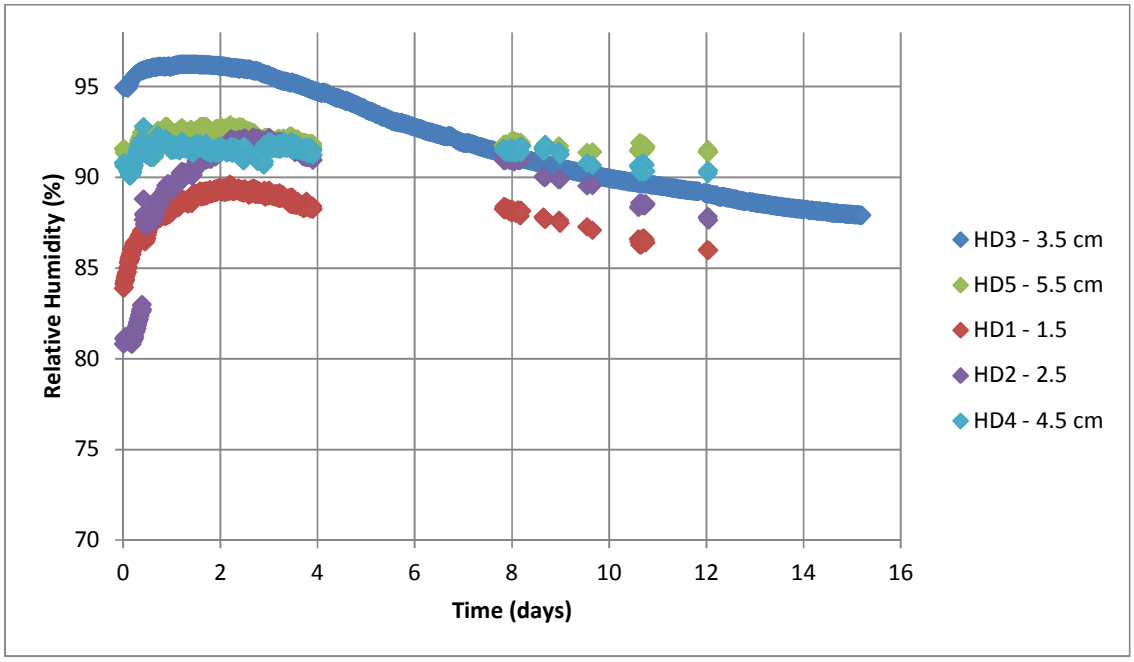


Fig. 85. RH readings at different depths for specimen D

The objective of the measurement was to obtain an internal moisture distribution and also to compare the results with the VAISALA measurements in specimen C. As stated before, this comparison is not possible as the VAISALA malfunction ruined it.

Regarding the readings for this specimen, it is observed that a high RH values were achieved in a short period of time: an average of 90% ± 3% due to the accuracy of the sensors for the Honeywell sensors (HD1, HD2, HD4, HD5); and 96% ± 3% for the Sensirion sensor (HD3). These values were expected comparing with the readings from the literature. At the day 10, the drop in the measurements was also as expected: a gradient of –2% for the deeper point (5.5 cm) and a higher gradient of – 4% for the point closer to the drying surface. There is a certain discontinuity at the day 8 that could be due to the sensors accuracy and the calibration of the Datataker DT 80G. However, HD3 did not present discontinuity. As mentioned before, the Sensirion Dattalogger presented more stability during the experiments.

5.3.4 Gravimetric Test

The following table shows the results of water content in the specimens at 7, 14 and 28 days.

Table 14. Water content for the gravimetric test

Gravimetric test								
			After 24 h	After 48 h			Date	
Specimen	Depth (cm)	Initial Weight (g)	Weight (g)	Weight (g)	Water content (g)	days	8/9/2011 10:00	Casting
G1	3	534	509	-	25	7.00	8/16/2011 10:00	
	6	590	562	-	28	7.00	8/16/2011 10:00	
	9	589	561	-	28	7.00	8/16/2011 10:00	
	12	668	638	-	30	7.00	8/16/2011 10:00	
	15	772	742	-	30	7.00	8/16/2011 10:00	
G2	3	594	569	-	25	14.00	8/23/2011 10:00	
	6	593	565	-	28	14.00	8/23/2011 10:00	
	9	566	539	-	27	14.00	8/23/2011 10:00	
	12	654	626	-	28	14.00	8/23/2011 10:00	
	15	695	666	-	29	14.00	8/23/2011 10:00	
G3	3	655.3	630.5	629.6	24.8	29.04	9/7/2011 11:00	
	6	621.7	594.6	593.8	27.1	29.04	9/7/2011 11:00	
	9	620.7	591.1	590.4	29.6	29.04	9/7/2011 11:00	
	12	591.0	561.0	561.0	30.0	29.04	9/7/2011 11:00	
	15	568.4	544.0	543.8	24.6	29.04	9/7/2011 11:00	

More time was required to get accurate conclusions, but a tendency to decrease the water content can be observed at 9, 12 and 15 cm depth. However, it was demonstrated that the use of this technique can be considered feasible for moisture content profiling.

The Fig. 86 Fig. 86. Moisture loss tendency for the gravimetric testshows the moisture loss tendency:

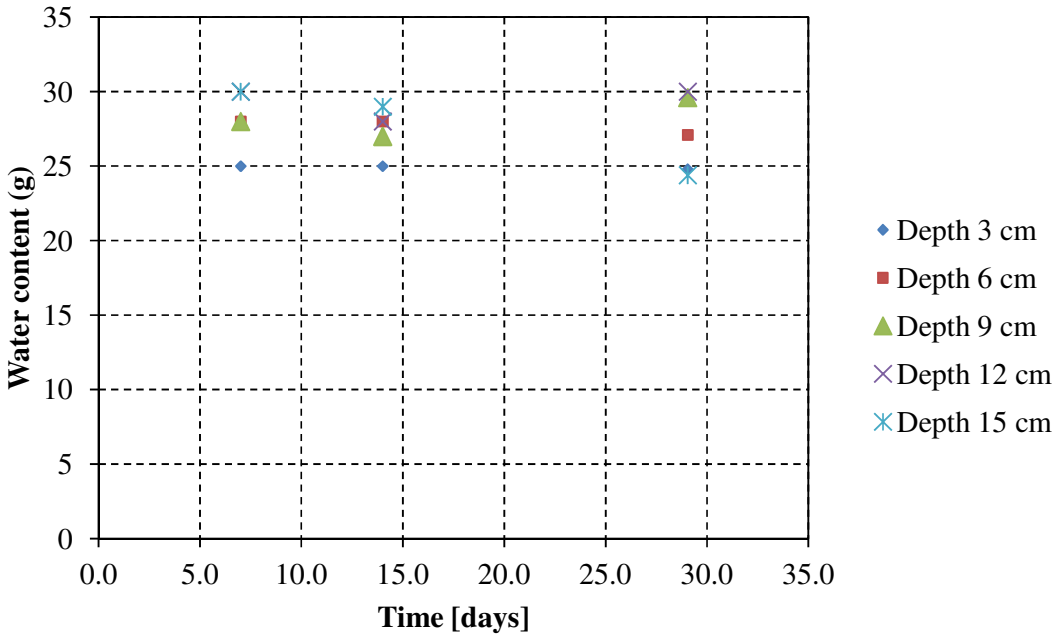


Fig. 86. Moisture loss tendency for the gravimetric test

5.3.5 Paradela Specimen

Before the experiments showed in the previous section, a preliminary test was performed in the same climatic chamber at 60%RH and 25°C, using a concrete specimen with the same dimensions (15x15x60 cm^3) but different number of drying surfaces (2 drying surfaces instead of 1 as in the Specimens A, B, C and D). The objective of showing the results (see Fig. 87) is not for comparison but to show the behaviour of internal moisture distribution in a longer period of time (3 months instead of 1 month). The concrete specimen was casted in the Paradela DAM and then brought to the climatic chamber in the laboratory. The sensors that were used are Sensirion sensors STH21. It was not possible to access to the concrete mix information.

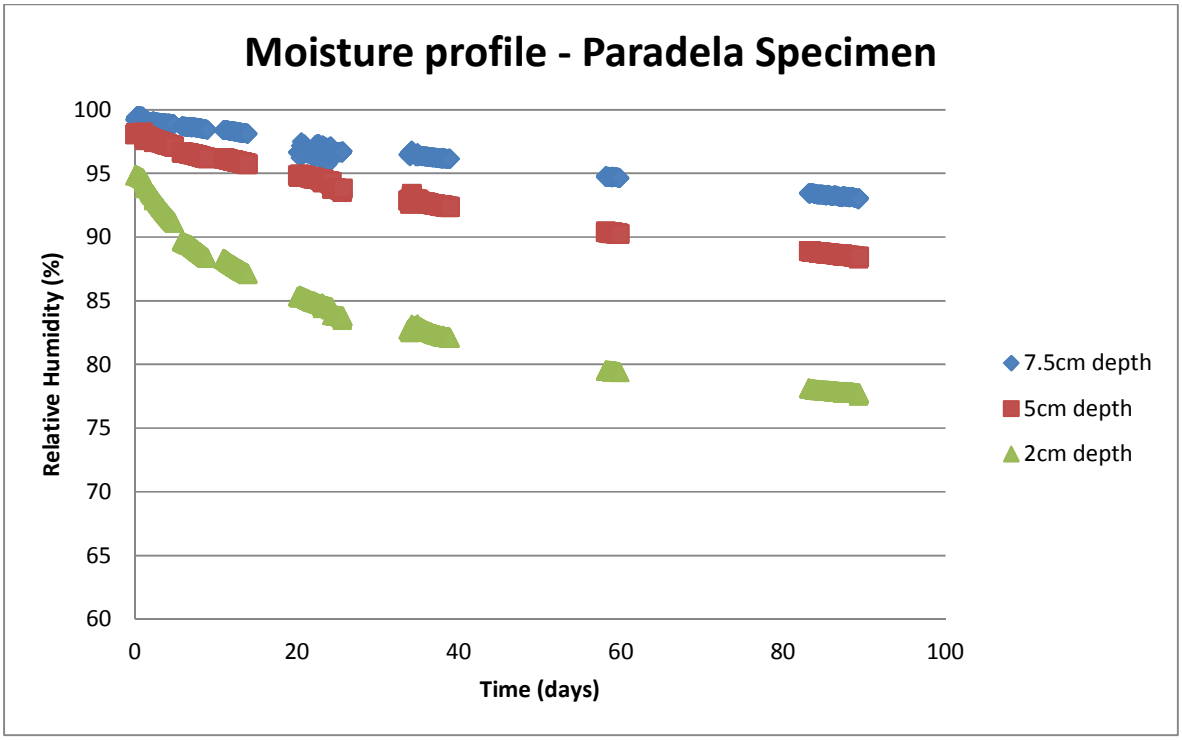


Fig. 87. Three months RH readings for the specimen with the concrete used in Paradela DAM

These results are more similar to the results presented by other authors in the literature review, with humidity values near to 100% right at the beginning. Then, the relative humidity gradients are around - 12% for the point nearest to the surface after 90 days in a continuous way; and a lower gradient of - 6 % at the deepest point in a continuous way, also as expected. The sensor at the middle depth gives a gradient of – 8%, closest to the deeper point. It is important to consider than the moisture flow is in 2 directions, the similar behavior with specimens with 1 drying surface could be because he RH sensor will be more sensitive to the moisture loss in the direction opposite of which the depth is considered. The fact that the specimens A and B did not present a high RH right at the beginning could be due to a bad isolation of the latex plugs.

6 CONCLUSIONS

It was feasible to measure the internal moisture distribution for concrete specimens using RH sensors and have a better understanding of their operation and behaviour under different environments. The experiments developed in this research work helped to do actual measurements inside concrete without damaging the RH sensors and with a minimum effect on the moisture content of the specimen.

Previous moisture loss profile measurement methods from different authors were identified and analyzed in order to choose the most accurate for this research work in terms of cost, availability of materials and accessibility to the required equipments. The lessons learned and the limitations of their work were considered and some of their assumptions verified, such as the effectiveness in the use of Gore-Tex for sensor protection (and the impact on the monitored RH), the accuracy of the sensors and their capacity to endure elevated humidity conditions for significant periods of time.

The possibility of creating controlled environmental conditions using salt solutions was studied with favourable results. Using simple containers that are commercially available, and salt compositions that were not specifically designed for environmental control, it was possible to create constant relative humidity conditions along time.

Different values of relative humidity could be reached and the performance of the salts could be analysed. At the same time, it has been of relevance to compare and to check the RH sensors performance. Reaching stability of sensor readings at very low and at very high RH values was difficult because of the lack of stability of salt solutions and the accuracy problems of the sensors at these extremes. It is common that RH sensors have limitations reaching

relative humidity below or near 10% RH, and above 90% RH, as it was observed on the performed measurements in containers with humidity controlled by salt solutions. Regarding this, it was confirmed that the larger the container the more salt would be necessary to reach a stable environment. A good practice or visual technique to achieve stability is to cover the base of the container with at least 3 mm of the salt solution.

Then, as observed in the results for the containers with cooking salt (NaCl), it is feasible to achieve constant RH with this kind of cheap/common salt. This opens the possibility to create homemade controlled environments when there are no other resources.

Finally, the glasses of water placed inside the containers caused the relative humidity values to increase. This effect was however weaker in the containers that had more quantity of salt solution. This shows that this effect can even disappear or be almost negligible by using high quantities of salt in the solution.

The testing of concrete specimens subjected to different relative humidity in a controlled environment could be feasible with a wide range of options that consider volume, size of the specimen and a specific value of relative humidity.

Regarding Gore-Tex, its use is feasible for moisture measurements inside concrete. However, special procedures have to be made to obtain accurate results as explained in this document. According to the obtained results it would be advisable to use Gore-Tex in a normal fashion to avoid the water to enter in the sensor case. However, an accurate sealing procedure as the one used for this research work, or equivalent, is required to achieve this target. Silicone worked well as a fixing and sealing material.

From the experience of this research, the option of wrapping the sensor directly with Gore-Tex seems not to be accurate for measurements in concrete. The sensors are usually very fragile and just having Gore-Tex clothes as protection would not be enough in an aggressive environment such as inside concrete.

About the differences in the readings when using Gore-Tex, they were not meaningful when measuring in the environment. The differences in all the cases have been less than 2.5%RH

which is in the range of the sensor´s accuracy. However, after the sensors were protected with Gore-Tex and PVC tube and subjected to extreme humidity environments (glass of water) the readings remained slightly higher even after stabilization. On this regard, it can be recommended to do not use sensors that have been exposed to high RH environments when accurate measurements are required. From an aggressive environment (around 95% to 100%RH), such as inside fresh concrete, changing the sensor to a moderate environment (around 45% to 65%RH) the gradient of RH is too high, and the sensors response may be biased by the previous environmental condition (loss of calibration). In this case, when the sensor was exposed to a 60%RH environment after being in a 100%RH environment, this 40%RH gradient affected the accuracy of the sensor, causing a tendency to give within 2% to 3% higher values.

For the experiments with the concrete specimens, an accurate procedure to prepare the specimens and place the RH sensors inside the concrete at the desired depth could be established. This is an important achievement for the scope of this research work, where feasible ways of measuring relative humidity inside concrete had to be found. No drilling was necessary, there was not additional moisture transfer with the environment thanks to the latex sealing in the PVC tubes. Furthermore, the latex sealing allowed small pocket sizes to be achieved (from 1.5cm to 3cm), and the sensors could provide accurate measurements for long periods of time. Despite of technical problems for some specimens, more than 3 months of measurements were possible (case of Paradela specimen) and the moisture loss profile could be obtained.

For the rest of variables, such as the influence of the pocket size in RH measurements and the comparison of the moisture profiles obtained with the gravimetric test, the results did not allow to get relevant conclusions. Certain tendencies and behaviors could be observed, but the time frame and some technical issues during the experiments avoid doing an accurate analysis. However, valuable knowledge could be obtained in terms of the procedures and potential sources of error.

7 REFERENCES

Akita, H. (1996). " A practical procedure for the analysis of moisture transfer within concrete due to drying." Magazine of Concrete Research **48 (6)**: 129-137.

Baroghel-Bouny, M. M., T. Lassabatere, O. Coussy (1999). "Characterization and identification of equilibrium and transfer moisture properties for ordinary and high-performance cementitious materials." Cement and Concrete Research **29**: 1225-1238.

Baroghel-Bouny, V. (2007). "Water vapour sorption experiments on hardened cementitious materials. Part II: Essential tool for assessment of transport properties and for durability prediction." Cement and Concrete Research **37**(3): 438-454.

DeAngelis, K. M. (2007). "Measurement of soil moisture content by gravimetric method." American Society of Agronomy: 1-2.

Devres, Y. O. (1994). "Psychrometric properties of humid air: Calculation procedures." Applied Energy **48**(1): 1-18.

Gatley, D. P. (2005). "Understanding Psychrometrics, 2nd ed.".

Herrmann S., H. J. K. (2009). "Thermodynamic properties of real moist air." HVAC&R Research.

J.C. Amba, J. P. B. (2010). "Characterisation of differential shrinkage of bonded mortar overlays subjected to drying." Materials and Structures **43**: 297-308.

Jensen, V. (2003). "Relative humidity measured by wooden stick method in concrete structures: long term measurements and reduction of humidity by surface treatment." Norwegian Concrete and Aggregate Laboratory: 1-13.

John Newman, B. S. C. (2003). "Advanced Concrete Technology : Concrete Properties." Butterworth-Heinemann **1**: 5-11.

Kharagpur (2002). "Introduction to Psychrometry " ME **Version 1**.

Kuehn, T. H. (1998). "Thermal Environmental Engineer (3rd edition ed)." New Jersey: Prentice Hall.

Kurumisawa, K. and K. Tanaka (2006). "Three-dimensional visualization of pore structure in hardened cement paste by the gallium intrusion technique." Cement and Concrete Research **36**(2): 330-336.

Li Chunqiu, L. K. (2008). "Numerical analysis of moisture influential depht in concrete during drying wetting cycles." Tshingua Science and Technology **Vol 13, N°5**: 696-701.

Norris, A., M. Saafi, et al. (2008). "Temperature and moisture monitoring in concrete structures using embedded nanotechnology/microelectromechanical systems (MEMS) sensors." Construction and Building Materials **22**(2): 111-120.

Parrott, L. J. (1990). "A review of methods to determine the moisture conditions in concrete." British Cement Association.

S. Multon, E. M. (2004). "Water distribution in beams damaged by alkali-silica reaction: global weighing and local gammadensitometry." Materials and Structures **Vol. 37**.

Selih, J. (1994). "Movement of water during drying of fully saturated concrete." PhD thesis, University of New Brunswick, Canada.

Selih, J., Antonio Sousa (1996). "Moisture transport in initially fully saturated concrete during drying." Transport in Porous Media **24**: 81-106.

Seungwook Lim, J.-H. J. (2009). "Moisture profiles and shrinkage in early-age concrete pavements." International Journal of Pavement Engineering **Vol. 10, N°1**: 29-38.

Villain, G. and M. Thiery (2006). "Gammadensimetry: A method to determine drying and carbonation profiles in concrete." NDT & E International **39**(4): 328-337.

Wiederhold, P. R. (1997). "Water vapor measurement, methods, and instrumentation." Marcel Dekker, Inc. New York: 384.

www.conservationphysics.org (2010). "Relative humidity sensors

": 1-3.

www.sensirion.com (2009). "Sensirion Sensors SHT Data Sheet - Version 04."

www.vaisala.com (2006). "VAISALA´s Relative Humidity Calibrator Users Guide."

Zachary Grasley, D. A. L. (2006). "Relative humidity in concrete." ACI Committee 236: 51-57.